Lawrence Berkeley National Laboratory
Recent Work

Title
Environmental Research Program - 1993 Annual Report

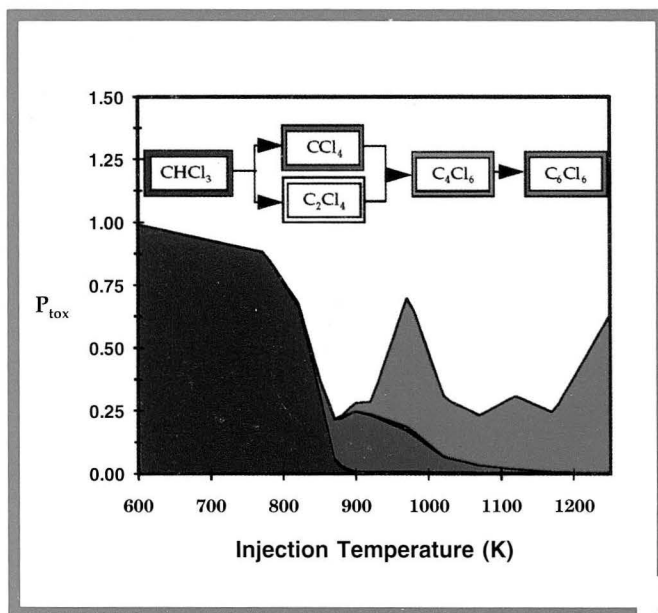**Permalink**
https://escholarship.org/uc/item/08w817sh

Author
Cairns, Elton

Publication Date
1994-06-01

Environmental Research Program

1993 Annual Report

Energy & Environment D
Lawrence Berkeley Lab(
UNIVERSITY OF CAL

DISCLAIMER

Environmental Research Program
1993 Annual Report

Nancy J. Brown, Program Head

Contents

Introduction

Flue-Gas Chemistry

Combustion

Atmospheric Aerosol Research

Ecological Systems

Introduction ████████████████████████

The objective of the Environmental Research Program is to contribute to the understanding of the formation, mitigation, transport, transformation, and ecological effects of energy-related pollutants on the environment. The program is multidisciplinary and includes fundamental and applied research in chemistry, physics, biology, engineering, and ecology. The program contributes research and development in efficient and environmentally benign combustion, pollutant abatement and destruction, and novel methods of detection and analysis of criteria and noncriteria pollutants. This diverse group conducts investigations in combustion, atmospheric and marine processes, flue-gas chemistry, and ecological systems.

Research in combustion science focuses on acquiring a fundamental understanding of the chemical and physical processes which occur during combustion for the purpose of optimizing the tradeoff between reducing emissions and increasing efficiency. Areas of application include engines, power generation, fire research, pollu-

tion abatement, and thermal destruction of wastes. Models have been developed to explore methods of reducing oxides of nitrogen for natural-gas combustion processes and to add chemistry to algorithms of turbulent reacting flow so that minor species (pollutants) can be predicted. Parametric and functional sensitivity analysis studies of potential energy surfaces have been undertaken to extract fully the physical content from dynamics-kinetics modeling efforts. Novel diagnostics have been developed to aid in the investigation of the interaction between turbulence and combustion. A weak-swirl burner has been developed to aid in the investigation of the interaction between turbulence and combustion. The burner is an ideal configuration for studying turbulent flame speed and flame quenching and supports combustion in very lean fuel conditions. A prime candidate for technology transfer, a production prototype is currently being developed for use in water heaters.

Studies investigating the thermal destruction of chlorinated hydro-

carbons have gained a more fundamental understanding of the chemical processes involved, enhanced methods for destroying these compounds while converting them to less toxic forms, and developed new diagnostic methods for the measurement of these species and their byproducts. While continuing to develop laser photofragmentation/laser-induced fluorescence techniques and *in situ* FTIR techniques for examining chlorinated species, substantial progress has been made in understanding the chemistry that occurs in combustion of chlorinated hydrocarbons. Developing other techniques for destroying or treating toxic waste is also an important research focus. Yellow phosphorus in the presence of moist air has been demonstrated to initiate chemistry that is effective in destroying various toxic organic compounds. The process is being optimized for both destruction efficiency and effectiveness of yellow phosphorus utilization.

Bioremediaton for the removal of toxic substances and, in particular, heavy metals is a growing area of

(cont.)

████████████████ Program Staff ████

Nancy J. Brown*, *Program Head*

Lisa Alvarez-Cohen	Charles Flesichmann	Revital Katznelson	Robert Risebrough
Susan Anderson	Stephanie Frolich	Jay Keasling	Carlos Rivera-Carpio
Frank Asaro	Ian Fry	John Knezovich[†]	C. Fred Rogers[†]
Benoit Bédat[†]	Jeronimo Garay	Catherine Koshland	Walter Sadinski
Kimberly Brouwer[‡]	Stephen Gehlbach[‡]	Larry Kostiuk	Robert Sawyer
Bob Buchanan	Robert Giauque	Michael Lee[‡]	Richard Schmidt
Steven Buckley	Gloria Gill	Shuncheng Lee	Ian Shepherd
Cheong-Ki Chan	Janet Gomez[†]	Terrance Leighton	Yao Shi[†]
Honkai Chang[‡]	Elisabeth Gray[†]	He Li[†]	Martyn Smith
Johnny Chang	Ralph Grief	David Littlejohn	David Steichen, Jr.
Melody Chang[‡]	Robert A. Harley	Donald Lucas	Fred Stross
Shih-Ger Chang*	John Harte	Robert Macey	Clement Sun[‡]
Jyh-Yuan Chen	Inge Hjelkrem[†]	John Maguire	Lawrence Talbot
Robert Cheng	Erika Hoffman	Qian-Hong Mao[†]	Chang-Lin Tien
Lloyd Connelly	Jennifer Hoffman	Samuel Markowitz	Shu-Mei Wang[†]
Robert Dibble	Jack Hollander	Andrew Maxson	Mark Wilcutts
Sophia Drugan[†]	Kenneth Hom	Rolf Mehlhorn	Gillian Wild
Rachel Dualan[†]	Ke-yuan Hu[†]	Marshal Merriam	R. Brady Williamson
Stephan Engleman[†]	Gary Hubbard	Katherine Moore	Michelle Wilson[‡]
Drazen Fabris	Mary Hunt	Tihomir Novakov*	Linda Wroth
Carlos Fernandez-Pello	John Jelinski	Antoni Oppenheim	Yi-Ran Wu
	David Jenkins	Lester Packer	Camillia Yang[‡]
*Group Leader	Yun Jin[†]	Patrick Pagni	Qi-Quan Yu†
[†]Participating Guest	Heeseung Kang	Erick Pham	Ya-Hui Zhuang[‡]
[‡]Student Assistant			

Introduction *cont.*

research. Bioremediation techniques are being developed for the characterization and decontamination of polluted environments. Novel assays using electron spin resonance (ESR) play an important role in understanding the processes involved. Biomass from microalgae and metabolically active bacteria are being used to remove and possibly recover heavy metals from water and soil. A related effort is recovering colorants from dye baths, which is of immediate interest to the textile industry.

Research in flue-gas chemistry investigates new processes for SO_2, NO_x, and CO_2 removal from gas streams and subsequent conversion to commercial feedstocks. Research begins by studying the fundamental reaction kinetics and integrating these results to devise a process at the laboratory scale which is further tested at the bench scale. Subsequent vital steps in the hierarchy leading to commercial development are pilot plant testing and demonstration-scale evaluation. A process involving a novel oxidation approach for the combined removal of SO_2 and NO_2 from flue gas has been successfully tested in conjunction with an industrial vendor. Another novel process involving a second-generation metal chelate for combined removal of both SO_2 and NO_x has been developed. This process avoids the production of unwanted byproducts which occur when conventional metal chelates are

used. An integrated bench-scale test of this process is in progress. Because large amounts of sulfur dioxide are produced from power plants, disposal of the products associated with its removal are often a problem. In response to this, an effective catalytic process has been developed for the reduction of SO_2 by synthesis gas to elemental sulfur, a valuable feedstock. Scale-up tests of this catalytic process with an industrial vendor are ongoing. Various catalysts have been tested for their efficacy in reducing CO_2 to elemental carbon.

Aerosol and cloud chemistry studies are a major area of emphasis. At present, the influence of atmospheric aerosols on global and regional climate is being studied. We have started to test the hypothesis that anthropogenic aerosols may mask, to some extent, the effects of increasing concentrations of "greenhouse" gases. Such an hypothesis assumes that there is a one-to-one relationship between cloud condensation nuclei and sulfate mass concentration and that anthropogenic sulfate is the principal aerosol species. Our research conducted at El Yunque Peak in Puerto Rico has demonstrated that the process is far more complex; the sensitivity of cloud droplet concentrations to changes in sulfate mass concentation is lower than previously assumed. Furthermore, we have found that organic aerosols contribute significantly more than do sulfate aerosols to

the number concentrations of particles that serve as cloud condensation nuclei.

Research in ecological systems is concerned with developing new tools for risk assessment. Bioassays and biophysical indices are used to elucidate environmental stress at the whole-animal and cellular levels. A bioassay that evaluates effects of contaminated soil, sediment, and pore water on reproduction of the soil nematode was found to be a practical method for assessing the impacts of a variety of contaminants. The importance of multigenerational exposures to UV(B) and chemical mutagens was investigated using the nematode animal model. Genotoxic effects of UV(B) were also evaluated in the Antarctic sea urchin. Another test allows detection of magnetic chromium species in living cells, which permits the study of mechanism of reduction of carcinogenic hexavalent chromium to more benign species. Marine studies have examined the chemistry and thermodynamics of anoxic environments throughout the geological record as a means of exploring the changing marine environment and its effect on mechanisms and kinetics of climate control. A study has been initiated to investigate the thermodynamics of gas hydrates under natural conditions as a means of assessing the contribution of gas hydrates to climate regulation, their potential as a resource of natural gas, and their potential as geohazards.

Flue-Gas Chemistry

Catalytic Reduction of Sulfur Dioxide to Elemental Sulfur

Y. Jin, Q. Yu, S.G. Chang

A number of regenerable flue gas desulfurization processes are under development. The processes are based on absorption of sulfur dioxide in the flue gas by an alkaline solution or a solid substrate. The sulfur dioxide is then stripped from the absorbant for treatment. It is desirable to convert the SO$_2$ to elemental sulfur, which has greater commercial value. In the presence of a catalyst, sulfur dioxide can be reduced with either synthesis gas or methane:

$$.875\ SO_2 + .75\ H_2 + CO \rightarrow$$
$$.438\ S_2 + CO_2 + .75\ H_2O \quad (1)$$

$$2\ SO_2 + 3\ H_2 + CO \rightarrow S_2 + CO_2 + 3\ H_2O \quad (2)$$
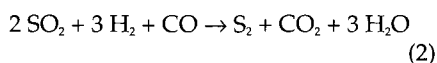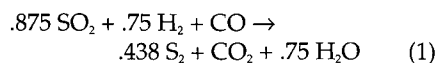
There are a number of undesirable side reactions that produce compounds such as H$_2$S, COS, CS$_2$, and elemental carbon. These reactions need to be minimized while allowing reactions (1) and (2) to proceed at high yield. It is desirable to have the catalyst operate at low temperatures and high flow conditions (high space velocity). It is also important for the catalyst to have a long and useful life.

We have developed a promising catalyst that is a combination of several metal oxides on a γ alumina support. The catalyst does not use any precious metals. The ratio of active catalyst material to substrate is about 0.3 by weight. Support sizes of 30-40 mesh and 3 mm dia. $\times$ 5 mm high were used. The catalyst was tested by flowing a gas mixture containing SO$_2$, H$_2$, and CO through a heated reactor containing the catalyst. The reacted gas mixture was analyzed by gas chromatography.

The catalyst material was tested over a temperature range of 340-580°C and a space velocity range of 1,000-15,000 per hour Measurements were made with [H$_2$ + CO]/[SO$_2$] varied from 1.4 to 3.0 and with [H$_2$]/[CO] at 0.4, 0.75, and 3. The efficiency for the conversion of SO$_2$ to elemental sulfur was determined over a range of operating conditions. The catalyst also was operated continuously for 1080 hours at temperatures of 440-480°C and a space velocity of 10,000/hr to determine its stability.

It was found that the catalyst could achieve greater than 90% conversion of SO$_2$ to elemental sulfur over a range of conditions. The optimum [H$_2$ + CO]/[SO$_2$] ratio was 2.0 at 480° C and 2000/hr space velocity. The SO$_2$ conversion was highest with [H$_2$]/[CO] of 3 at a space velocity of 10,000/hr over a range of temperatures, although it was only slightly better than the conversion at a ratio of 0.75. Higher sulfur dioxide conversions were obtained at higher temperatures. The conversion leveled off at the highest temperatures studied. SO$_2$ conversions increased as the space velocity decreased, with the conversion leveling off at the lowest space velocity. The effect of space velocity on SO$_2$ conversion was very sensitive to the catalyst particle size. The 30-40 mesh catalyst support was much less sensitive to space velocity than the catalyst on the larger particles.

The catalyst showed essentially no deterioration over the period of the the lifetime test. The new material promises to be superior to the Claus process in converting sulfur dioxide to elemental sulfur with the capability to achieve greater than 95% conversion in a single-stage reactor.

Removal of NO from Flue Gas with Ferrous Dimercaptopropane Sulfonate

E.K. Pham, S.G. Chang

Nitric oxide (NO) is the predominant nitrogen oxide in flue gas and is relatively insoluble in aqueous solutions. Consequently, it is difficult to remove from flue gas with wet scrubber systems. Ferrous ion complexes are often added to aqueous scrubbing solutions to improve the removal of nitric oxide by the formation of ferrous nitrosyl complexes. While these compounds are effective in removing nitric oxide, they suffer from sensitivity to residual oxygen in the flue gas and tend to react with dissolved sulfur dioxide to form undesirable compounds. We report here a new complex based on 2,3-dimercapto-1-propane sulfonate (DMPS) which is effective in removing NO and avoids the problems associated with other complexes.

DMPS and Fe^{2+} form a 2:1 complex in aqueous solution that has a large capacity for NO over a wide pH range. The absorption capacity of Fe^{2+}(DMPS)$_2$ was compared with Fe^{2+}(EDTA) at 55°C by bubbling simulated flue gas containing 580 ppm NO through 10 mM solutions at pH 6.6. In the absence of oxygen, the Fe^{2+}(DMPS)$_2$ solution formed 7.5 mM nitrosyl complex whereas Fe^{2+}(EDTA) absorbed only 2.6 mM. When 5% oxygen was added to the gas stream, the difference was more significant. Fe^{2+}(DMPS)$_2$ formed 3.3 mM of the nitrosyl complex, and Fe^{2+}(EDTA) formed only 0.44 mM nitrosyl. The improved performance of the Fe^{2+}(DMPS)$_2$ complex in the presence of oxygen is due to the ability of DMPS to rapidly regenerate ferrous ion from ferric ion. In reducing ferric ion, DMPS is converted to its oxidized form with an S-S linkage. In our earlier studies of ferrous thiochelate complexes, we found that addition of the ligands beyond stoichiometric ratios improved performance by continued reduction of ferric ion. However, addition of DMPS beyond stoichiometric quantities did not improve absorption of nitric oxide in the presence of oxygen.

Fe²⁺(EDTA)NO can be regenerated by allowing it to react with dissolved sulfur dioxide. However, this reaction produces a number of undesirable products including nitrous oxide and nitrogen-sulfur compounds. $Fe^{2+}(DMPS)_2NO$ does not react with sulfite or hydrogen sulfite ions so there is no problem with generation of these compounds.

Thermal regeneration and electro-regeneration were both investigated as methods to regenerate the $Fe^{2+}(DMPS)_2NO$ solution. Thermal regeneration is appealing because it only requires heating the solution in the absence of oxygen to release nitric oxide. Solutions of $Fe^{2+}(DMPS)_2NO$ were heated at 100°C for up to two hours to drive off the bound NO. The solution was then treated with dilute NO in N_2 to determine the degree of regeneration. It was found that only 7% of the NO was released during the heat treatment. The regeneration was reproducible over a number of cycles. Electroreduction of $Fe^{2+}(DMPS)_2NO$ appears to be an effective technique. Cyclic voltammetry of $Fe^{2+}(DMPS)_2NO$ solutions shows a wave due to NO reduction at -0.75 V relative to SCE. Reduction of the oxidized DMPS S-S linkage occurs at a similar potential. Solutions of $Fe^{2+}(DMPS)_2NO$ have been electroreduced using glassy carbon and platinum electrodes with current densities of 15-20 mA/cm². Analysis of the solutions indicates that the conversion of NO to NH_3 is quantitative.

The $Fe^{2+}(DMPS)_2$-based flue-gas scrubbing solution appears to be superior to conventional ferrous chelate solutions in its high absorption capacity, resistance to oxidation, and in the absence of undesirable byproducts.

The PHOSNOX Process for Removal of SO₂ and NOₓ from Flue Gas

S.M. Wang, S.G. Chang

The PhoSNOX process for combined removal of sulfur dioxide (SO₂) and nitrogen oxides (NOₓ) has been shown to be a promising technique for treating flue gas from coal-fired power plants. We report here results from additional studies of the process. The process generates a mist of phosphoric acid droplets. We have investigated the particle size distribution of the phosphoric acid mist generated by the interaction of air with the aqueous phosphorus emulsion. The droplets need to be removed from the gas stream to recover phosphoric acid and to avoid opacity problems with the exhaust plume. The most effective removal technique depends on the particle size distribution of the mist. Measurements were made with a laser optical particle counter and with a cascade impactor system. The optical particle counter measured the mist in terms of mass frequency *vs.* size. The two techniques provided results that were in good agreement with one another.

The size of the mist droplets increases with the residence time in the gas stream. This is believed to be due primarily to coagulation. There is some decrease in temperature of the mist as it flows so some size increase could be due to condensation as well. The size distribution measurements from the two techniques are tabulated (Table).

The size distribution of the mist peaked at 0.5 mm, 0.9 mm, and 1.1 mm at the respective residence times of 0.7 sec, 6.5 sec, and 11.2 sec.

The concentration of phosphoric acid in the mist droplets was determined by collecting the droplets on a sintered glass impactor. The liquid collecting on the sintered glass plate was sucked through a capillary tube to a collection reservoir. The solutions were analyzed by comparison with solutions of known concentration using ion chromatography. The mist droplets were found to be about 10% phosphoric acid by weight.

From the results of this study, it appears that a submicron mist collector such as an Aerosep multistage aerosol separation system may be needed to recover the mist droplets in commercial scrubbers. The residence time of the mist in a prescrubber or scrubber is expected to be less than five seconds so a substantial fraction of the mist droplets will be less than 1 mm. The recovered acid will need to be concentrated to about 75% by weight for the commercial market.

Table. *Size of phosphoric acid particles in experimental mist*

Measurement Technique	Residence Time			
	0.7 sec	2.8 sec	6.5 sec	11.2 sec
Laser optical particle counter	0.66 mm	0.72 mm	0.97 mm	1.10 mm
Cascade impactor	0.67 mm	0.67 mm	0.83 mm	-

Methanation of CO₂ with Activated Ni(II)- and Co(II)-Bearing Ferrites

T. Kodama, S.G. Chang

Whereas the hydrogenation of carbon monoxide (CO) has been studied extensively, little work has been done on the hydrogenation of carbon dioxide (CO₂). Results in the literature indicate that poor conversion and low selectivity have been obtained in the hydrogenation of CO₂ using Ru, Fe, and Co/SiO₂ catalysts. Tamaura and coworkers have previously investigated the decomposition of CO₂ on magnetite which had been activated by flowing hydrogen through it at 300°C. They have also studied the methanation of CO₂ on activated magnetite. Nearly 90% conversion was obtained at 300°C, although it decreased to 25-50% at 200°C.

In this study, we examined the methanation of CO₂ using ferrites containing Ni(II) or Co(II). The modified ferrites were prepared by air oxidation and precipitation of aqueous suspensions of Fe(II) hydroxide and either Ni(II) or Co(II) ions. The modified ferrite powder was placed in a temperature-controlled cell and activated by flowing hydrogen through at 300°C.

Following the activation, the cell containing the ferrite was evacuated, and carbon dioxide was added. The temperature was maintained at 300°C for 10 minutes while the CO_2 decomposed. The cell was again evacuated, and the temperature was lowered to 150-200°C. Hydrogen was again added to the cell. The gases in the cell after CO_2 addition and H_2 addition were analyzed by gas chromatography.

Analysis of the CO_2 adsorption isotherms indicates that the CO_2 adsorbs on the surface of the catalyst and decomposes to elemental carbon and two oxygen ions (O^{-2}). The results of the CO_2 conversion measurements are compared (Table).

The modified ferrites show improved CO_2 conversion compared to magnetite. No gas other than methane was observed from treating the catalysts with hydrogen following reduction of CO_2. Whereas both the Ni(II)-bearing ferrite and the Co(II)-bearing ferrite had higher conversions to methane than

Table. *Results of methanation of CO_2 using ferrites containing Ni(II) or Co(II).*

Sample	M(II)/Fe$_{total}$	% CO_2 Decomposition
Activated magnetite	0	86.4
Activated Ni(II) ferrite	0.050	97.7
	0.143	98.8
Activated Co(II) ferrite	0.045	86.8
	0.132	81.1
	0.262	96.9

magnetite, only the Ni(II)-bearing ferrite showed a substantial conversion to methane. With the Ni(II)-bearing ferrite, the conversion was proportional to the the fraction of Ni(II) present. The conversion of deposited carbon to methane for the Ni(II)-bearing ferrite (Ni(II)/Fe$_{total}$ = .143) at 300°C was 45.5% at 0.75 hr, 59.3% at 1.5 hr, and 86.9% at 3 hr hydrogen reduction time. The addition of transition metal ions to ferrite improved the efficiency of both carbon dioxide reduction and methane conversion. The Ni(II)-bearing ferrite had particularly high conversion efficiencies.

Reference

Tamaura Y and Tabata M. Complete reduction of carbon dioxide to carbon using cation-excess magnetite. *Nature* 1990; 346: 255.

Destruction of Toxic Organic Compounds with Yellow Phosphorus

S.M. Wang, S.G. Chang

There are many hazardous wastes sites in the United States that contain water or soil contaminated with toxic organic compounds. Many of these compounds are difficult to destroy due to their structure, and many of the treatment methods proposed for treatment of toxic organics, such as ozonation, UV irradiation, and plasma treatment, are costly. We recently developed a novel method for treatment of organic compounds based on the reaction of yellow phosphorus with oxygen in aqueous solution. The phosphorus oxidation process generates a number of phosphorus oxide intermediates as well as UV and visible light. The products of the reaction include oxygen atoms, ozone, and phosphoric acid.

Our studies were carried out in two types of reaction systems. In the first system, 100 mL of water with ppm quantities of the organic compound under study was added to a flask with 0.1-1.0 g phosphorus and stirred in contact with air at a temperature of 50-55°C. The second system consisted of a column heated to 50-55°C that contained 250 mL of the mixture of water, phosphorus, and the organic compound. Air was bubbled through the

column at 40-170 mL/min, and the solution was agitated with a series of reciprocating stainless steel screens. The mixture could be circulated by pumping it through a nozzle at the top of the column with a centrifugal pump if desired. The decomposition of the compounds was monitored by UV-visible spectroscopy, gas chromatography, and ion chromatography.

We studied a number of organic compounds, including naphthalene, chlorobenzene, Arochlor 1221, Eriochrome black T, dimethyl aniline, phenol, benzoic acid, nitrobenzene, isophorone, and pyridine. Survey measurements of the decomposition of the compounds were made in the stirring reactor. More detailed parametric destruction studies were made with the column reactor. The reactions were followed for several hours. All compounds were degraded by the treatment.

In some cases, the decomposition products of the process were determined. The organic compounds were generally converted into simple organic carboxylic acids such as formic, acetic, malonic, and oxalic acids. The rate of decomposition was highly dependent on gas-liquid contact. Spraying and agita-

tion were most effective in achieving high destruction rates. The rate of destruction was also proportional to the amount of phosphorus used and the air flow rate. The rate of destruction of the organic compound was also proportional to its concentration. Since the reaction system is quite complicated and involves gas-liquid mass transfer, simple linear relationships are unlikely to exist between rate of destruction and the experimental variables studied.

The yellow phosphorus oxidation technique appears to be a promising method for treating hazardous organic compounds. It is inexpensive, versatile, and effective on a wide range of organic compounds.
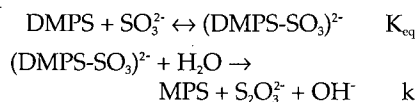
Reaction of Sulfite Ion with Dimercaptopropane Sulfonate

D. Littlejohn, S.G. Chang

We have been investigating dimercaptopropane sulfonate (DMPS) as a ligand to complex ferrous ion for use as a nitric oxide binding agent in wet flue-gas scrubbing systems. In the course of our investigations, it was found that DMPS slowly reacts with sulfite ions. Thiosulfate ion was detected in mixtures of the two compounds. Ion chromatography was used to monitor the build-up of thiosulfate and the loss of sulfite in the reaction mixtures. In the absence of ferrous ion, it was found that sulfite ion rapidly forms a complex with DMPS. The UV absorption spectrum of DMPS-sulfite solutions has a featureless absorption that starts at about 280 nm and increases to shorter wavelengths. The strength of the absorption levels off as the sulfite/DMPS ratio is increased suggesting the formation of a complex. When diluted, the absorbance decreases by an amount that would be expected by a reversible complex. The complex appears to decompose directly to the observed products, thiosulfate ion, $S_2O_3^{2-}$, and mercaptopropane sulfonate.

From the observed behavior, the reaction process can be written as:

$$DMPS + SO_3^{2-} \leftrightarrow (DMPS\text{-}SO_3)^{2-} \quad K_{eq}$$

$$(DMPS\text{-}SO_3)^{2-} + H_2O \rightarrow$$
$$MPS + S_2O_3^{2-} + OH^- \quad k$$

The DMPS appears to be converted to mercaptopropane sulfonate (MPS) on the loss of a sulfur to the sulfite to form thiosulfate. From the UV absorption measurements on DMPS-sulfite solutions, a value of $K_{eq} = 7 \pm 2$ M^{-1} was derived at 25°C and pH about 8. The ion chromatograph measurements were used to derive a value of $k = 1.9 \pm 0.6 \times 10^{-6}$/sec for the unimolecular decomposition of the complex. Measurements at 37°C and 50°C were used to determine the temperature dependence of the reaction. The activation energy for k was found to be $E_a = 15.9$ kcal/mol. The rate of the reaction is extremely slow at pH 4 and below and increases above pH 10. The increase is presumably due to the deprotonation of the mercapto groups on DMPS which would assist the reaction.

It was found that sulfite ion also reacts with three other compounds with dithio groups, dimercaptosuccinate, dithiooxalate, and dithiothreitol. Dithiothreitol has non-adjacent SH groups and reacts much more slowly than the other compounds. Measurements on mixtures of sulfite ion with cysteine, 2-aminoethanethiol, and 2-mercaptoethanesulfonate showed no evidence of reaction. All of the latter compounds have a single SH group.

The reaction of sulfite ion with DMPS bound to ferrous ion as $Fe^{2+}(DMPS)_2$ also shows evidence of the formation of a complex prior to reaction. DMPS bound to ferrous ion is somewhat more reactive below pH 6 and less reactive at higher pH than free DMPS in solutions of sulfite ion. The reaction products appear to be the same with or without ferrous ion.
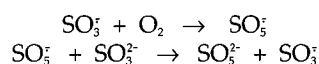
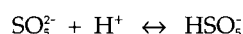## Reaction of HSO$_5^-$ with Sulfite and Hydrogen Sulfite Ions

D. Littlejohn

In our earlier study of the oxidation of hydrogen sulfite ions by molecular oxygen, we detected disulfate ion ($S_2O_7^{2-}$) as an intermediate. The mechanism of formation of disulfate ion had not been determined. Other studies have shown that sulfite radical is formed in the initiation step for S(IV) oxidation:

$$SO_3^{2-} + A \rightarrow SO_3^- + A^-$$
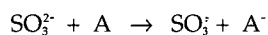
The sulfite radical can then react very rapidly with oxygen to form peroxymonosulfate radical, which can then react with sulfite ion.

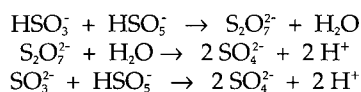$$SO_3^- + O_2 \rightarrow SO_5^-$$
$$SO_5^- + SO_3^{2-} \rightarrow SO_5^{2-} + SO_3^-$$

Peroxymonosulfate ion has a pKa of 9.88 so it exists as HSO_5^- in neutral and acidic solutions.

$$SO_5^{2-} + H^+ \leftrightarrow HSO_5^-$$

We studied the reaction of peroxymonosulfate ion, HSO_5^-, with sulfite and hydrogen sulfite ions to determine if this reaction could be responsible for the generation of disulfate ion in our earlier oxidation studies. A solution of the mixed potassium salt of hydrogen sulfate, sulfate, and peroxymonosulfate was combined with solutions of sodium metabisulfite and sodium sulfite.

Raman spectra of mixtures of HSO_3^- and HSO_5^- solutions showed a signal at 1090/cm where there is a disulfate ion band. Under stopped-flow conditions, the 1090/cm signal decayed and the 981/cm and 1050/cm signals of sulfate and hydrogen sulfate built up at the rate characteristic of disulfate ion hydrolysis. However, the 1090/cm signal was not observed in the reaction of SO_3^{2-} with HSO_5^-. This indicates that disulfate ion is formed from the reaction of hydrogen sulfite with peroxymonosulfate only.

$$HSO_3^- + HSO_5^- \rightarrow S_2O_7^{2-} + H_2O$$
$$S_2O_7^{2-} + H_2O \rightarrow 2SO_4^{2-} + 2H^+$$
$$SO_3^{2-} + HSO_5^- \rightarrow 2SO_4^{2-} + 2H^+$$

Observations were also made of the pH change during reaction to determine the number of hydrogen ions produced by the reaction. The pH change observed is consistent with the release of 2 H^+ per HSO_5^-. Connick and coworkers have also investigated the reaction of HSO_5^- with S(IV) and have proposed a mechanism that is consistent with our observations.

Reference

Littlejohn D, Hu KY, Chang SG. Oxidation of HSO$_3^-$ by O$_2$. *I&EC Research* 1988; 27: 1344.

Combustion

Thermal Destruction of Toxic Compounds

D. Lucas, R.F. Sawyer, C.P. Koshland, C. McEnally, M. Thomson, S. Lee, B.S. Higgins, S.G. Buckley, B. Lau

The disposal or treatment of hazardous wastes is a subject of widespread concern. Even with hazardous waste reduction, most waste management experts see a long-term requirement for hazardous waste disposal technologies. While incineration currently provides the highest available destruction efficiency for organic compounds, serious public concern remains as to the effects of thermal destruction techniques such as incineration. The goals of our research are to gain a fundamental understanding of the chemical processes that occur when chlorinated hydrocarbons are destroyed thermally, to study new ways to enhance the destruction of these compounds, and to develop new diagnostic methods for measuring these species and their byproducts.

We continue to develop nonintrusive optical diagnostics based on excimer laser fragmentation/fluorescence spectroscopy (ELFFS). Using the CCl radical as the detected fragment, we have measured chlorinated hydrocarbons at concentrations in the ppb range with a measurement time of seconds and in a sooting flame environment. These are the first spatially resolved *in situ* measurements of chlorinated hydrocarbons in flames.

We are also studying the thermal destruction of chlorinated hydrocarbons in a turbulent flow reactor with the CHCs injected as gases, liquids, or mixtures. We have developed a method for evaluating the toxicity of exhaust emissions using measured concentrations of all species including combustion byproducts weighted by a toxicity value which includes both carcinogenic and noncarcinogenic chronic health effects. If the waste were simply evaporated, the toxicity index would be 1. An example is shown (Figure) where we have used published data from the flow reactor of Dellinger et al. for the destruction of chloroform as a function of injection temperature.

The addition of small amounts of fuels to the post-flame combustion products can enhance the destruction of trace amounts of toxic species that persist in incinerator exhausts. We have added hydrocarbon fuels, methanol, and carbon monoxide. We determined that unimolecular reactions are not affected by fuel addition, but bimolecular rates are strongly influenced by the radical levels. For example, all fuels enhance the destruction of methyl chloride; CO is the only fuel that destroys ethyl chloride; and none of the fuels affect the destruction of trichloroethane.

References

Lee S, Koshland CP, Sawyer RF, Lucas D. Effects of post-flame fuel injection on the destruction of chlorinated hydrocarbons. *Combust. Sci. Technol.* (in press).

Lee S, Koshland CP, Sawyer RF, Lucas D. Enhanced destruction of chlorinated hydrocarbons in post-flame combustion gases. *Combust. Sci. Technol.* (in press).

McEnally, CS, Lucas D, Koshland CP, Sawyer RF. Sensitive *in situ* detection of chlorinated hydrocarbons in gas mixtures. *Appl. Optics* (in press).

Thomson MJ, Lucas D, Koshland CP, Sawyer RF, W Y, and Bozzelli, JW. An experimental and numerical study of the high-temperature oxidation of 1,1,1-trichloroethane. *Combust. Flame* (in press).

Thomson MJ, Higgins BS, Lucas D, Koshland CP, Sawyer RF. The mechanism of phosgene formation from 1,1,1-trichloroethane oxidation. *Combust. Sci. Technol.* (in press).
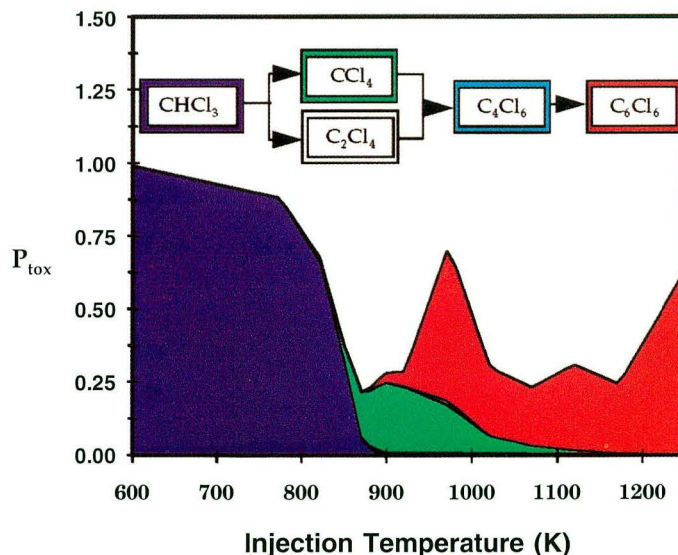

Figure. *The overall toxicity of an exhaust stream depends on the concentrations and toxicities of its individual components. P_{tox} is a toxicity index we have developed for combustion species. As the initial compound, chloroform in this example, reacts in a flow reactor, the toxicity can vary significantly from the initial value of 1.*

Controlled Combustion

J.A. Maxson, A.K. Oppenheim

According to current technological standards, combustion chambers for prime movers are treated solely as sources of power without much attention given to their performance as chemical reactors. Consequently, their tendency to produce air pollutants is relatively unconstrained. In the automotive industry, for example, the strategy adopted throughout the world to deal with the problem of pollutant emissions is to reduce their yield by chemical processing of combustion products in the exhaust system.

The basic purpose of our studies is to provide a scientific basis for controlling the combustion process so that the formation of pollutants is reduced. It turns out that the same means are beneficial to fuel economy—a prominent factor in reducing the CO_2 pollution—and engine tolerance to a wide variety of fuels—a significant aid in the logistics of fuel supply.

Our ultimate goal is advancement of the technology of internal combustion engines. For this purpose, the acquisition of knowledge on systems and processes in current use and the concomitant progress of science, albeit necessary prerequisites, are by themselves not sufficient. To be actually effective, this has to be supplemented by concepts and their assessment. After more than a decade of studies on the fundamentals of ignition and combustion of particular relevance to internal combustion engines, we are now entering the phase of the development and study of new concepts.

In the continuation of this program of research, we are now devising a rational approach to the evaluation of the thermochemical processes associated with the initiation and execution of the exothermic process of combustion in engines. The objectives of our current studies are:

- Provision of a fundamental background for estimating the consequences of a variety of modes in which the process of combustion can be executed—this concerns primarily Flame Traversing the Charge (FTC) following spark ignition as is typical of current technology in contrast to a Pulsed Combustion Jet system or PCJ leading to Fireball Mode of Combustion (FMC). We thereby expect to pave the way for the development of controlled, clean combustion engines of the future;

- Comprehensive rendition of the thermochemical processes of combustion in terms of integral curves (trajectories) in the phase (state) space to serve as conditions of constraint for the Computational Fluid Mechanics or CFM solution whereby the latter acquires the character of an eigenfunction problem in nonlinear mechanics;

- Formulation of the thermochemical nature of engine combustion as the object of an electronically governed control system;

- Derivation of solutions for inverse problems in engine combustion, that is, deduction of information on the execution of the exothermic process and the consumption of fuel and production of pollutants from measured pressure profiles expressed in terms of indicator diagrams.

The latter study was supported by the LBL Laboratory-Directed R&D Fund. The computational algorithm developed for this purpose consists of three consecutive steps: 1) thermodynamics, 2) thermochemistry, and 3) aerodynamics. From the first, one immediately gets information on the specific fuel consumption; from the second, an estimate is obtained on the formation of chemokinetically controlled pollutants, NO_x and CO, and from the third, guidelines are provided for the fluid mechanical control of the exothermic process of combustion pertaining, in particular, to the reduction of unburned hydrocarbon emissions.

The study yielded manuscripts for two papers: *Can the Maximization of Fuel Economy be Compatible with the Minimization of Pollutant Emissions*, for the 1994 Society of Automotive Engineering Congress; and *A Thermochemical Phase Space for Combustion in Engines*, for the 1994 International Symposium on Combustion as well as a project proposal on "Design Analysis for Optimal Execution of the Exothermic Process of Combustion in Natural Gas Fueled Engines" to be financed by contract with Southwest Research Institute.

The first paper provided arguments explaining the rationale for meeting President Clinton's mandate delineated by the Clean Car Initiative as doubling, at least, the mileage per gallon of fuel while simultaneously eliminating pollutant emissions with radical improvements in the execution of the exothermic process of combustion in engines—a task involving the transformation of the contemporary mode of FTC to microprocessor-controlled FMC, the epitome of Direct Injection Stratified Charge or DISC engine featuring late injection and stratified combustion using a PCJ system. It also introduces a systematic procedure for engine development consisting of thermodynamic and thermochemical computations that, with an aerodynamic analysis of the turbulent field, lays the groundwork for engine design by a systematic procedure of Indicator Diagram Tailoring or IDT.

The second paper introduced the concept of a thermochemical phase space based on the recognition that the combustion system is nonlinear and therefore utilizing the classical concept of nonlinear mechanics: a space whose coordinates are the dependent variables of the problem. In the case at hand, they consist of all the thermochemical parameters of the system. The dimension of this space is thus equal to the number of degrees of freedom. We name it the Le Chatelier Space. Its major asset lies in providing information, expressed in terms of trajectories or manifolds, on the global effects of the thermochemical processes that take place in the physical space of the combustion chamber. An analytical insight is thereby obtained into the effective mechanism of the exothermic process of combustion. Application of the method is illustrated by the evaluation of advantages one can accrue on this basis for a premixed charge engine. It is shown, in particular, that if, instead of a throttled homogeneous combustion, the exothermic process is executed in a FMC version of a PCJ-generated DISC system, the engine can be rendered the ability for part-load operation at wide open throttle with significant gains in fuel economy and concomitant reduction in pollutant emissions. Such a mode of combustion occurs within large-scale vortex structures generated and sustained by pulsed jets.

The proposal is offered to provide assistance in assessing and optimizing

the performance of natural-gas-fueled engines, emphasizing particular concern with the execution of the exothermic process of combustion—the crucial event associated with the production of motive force, consumption of fuel, and concomitant generation of pollutants that so far has been vastly overlooked in engine development and design.

References

Oppenheim AK. The future of combustion in engines. *Proceedings of the Institution of Mechanical Engineers* 1992; C448/022: 187.

Oppenheim A K. Life on Earth at the point of inflection. *Proceedings of the Institution of Mechanical Engineers* 1992; C448/076: 215.

Murase E, Ono S, Hanada K, Nakahara S, Endo H, Oppenheim AK. Combustion enhancement of lean mixture by plasma jet ignition and pulsed jet ignition. *Transactions of the Japan Society of Mechanical Engineers* 1992; 58: 561.

Gavillet GG, Maxson JA, Oppenheim AK. "Thermodynamic and Thermochemical Aspects of Combustion in Premixed Charge Engines Revisited." SAE Paper 930432, 1993.

Oppenheim AK, Maxson JA. Thermodynamics of Combustion in an Enclosure. In: *Dynamics of Heterogeneous Combustion and Reacting Systems.* AIAA Progress of Astronautics and Aeronautics, Vol. 152. Washington, D.C., 1993, pp. 365-382.

Oppenheim AK. Turbulent Combustion in Contrast to Flames. In: <u>Modern Developments in Energy, Combustion and Spectroscopy</u>. Pergamon Press, 1993, pp. 1-13.

Oppenheim AK, Maxson JA, Wilcutts MA, Faris DW, Packard AK, Hedrick JK. Fireball Mode of Combustion and Its Adaptive Control. In: <u>Twenty-Sixth International Symposium on Automotive Technology and Automation, Aachen, Germany, 1993.</u>

Combustion Fluid Mechanics

R.K. Cheng, I.G. Shepherd, L.W. Kostiuk, B. Bédat, L. Talbot

Turbulent combustion takes place in all heat and power generating systems. Its most important role is to increase the burning rate and volumetric power density. Turbulent mixing, however, also influences the chemical reaction rates of the combustion processes and has a direct effect on the formation of pollutants, flame ignition, and extinction. Therefore, research and development of modern combustion systems for power generation, waste incineration, and material synthesis must rely on a fundamental understanding of the physical effects of turbulence on combustion. Such knowledge is key to successful development of theoretical and computational models which can be used as design tools.

The overall objective of our research is to investigate the interaction and coupling between turbulence and combustion. These processes are highly complex and consist of scalar and velocity fluctuations spanning several orders of magnitudes. The geometry of the burner and the flame configuration also have a profound effect. Our approach to gain a fundamental understanding is by investigating laboratory flames with simple geometries that are amenable to detailed interrogation by laser diagnostics. These laboratory burners allow systematic variation of turbulence intensities and mixtures composition. Their flow geometries are chosen to simplify numerical modeling and simulations and to facilitate direct comparison between experiments and theory.

Our experiment has concentrated on flames with moderate turbulence intensity where chemical reaction rates are not significantly affected by turbulence mixing. The turbulent burning rate can be determined from the flame surface area that can be compared to the turbulence characteristics. Our goal is to extend the scope of the experiments to include flames with high turbulence intensity. These flames are closer to the combustion in practical systems. The effect of increased turbulence may include the reduction of burning rate and intermittent flame quenching and reignition. Studying these intense turbulent flames requires *in situ* measurement of the local burning rates. The steep scalar gradients across the reaction zone coupled with rapid flame motion makes the task quite challenging. The experience gained from investigation of flames with moderate turbulence is expected to provide the necessary scientific and theoretical background for this new research direction.

The principal characteristics of premixed turbulent flames is that the combustion processes are affected by boundary conditions upstream and downstream of the flame. Our strategy to solve this complex problem is to investigate flame propagation under a variety of flow geometries. We have thus far developed five laboratory flame configurations. These burners are designed to operate under a wide range of conditions so that the response of the flame to different turbulence inten-

sities and mixture equivalence ratios can be investigated systematically. Our first two configurations are simulations of those found in many practical systems. They are rod-stabilized v-flame propagating in turbulent flow and a large axisymmetric Bunsen-type conical turbulent flame stabilized by a pilot. The next two were developed because the flowfield and flame orientation are easy to model. They are planar flames stabilized in stagnation flows produced by a plate or by two opposed streams. The flames are locally normal to the approach flow and are stabilized without flow recirculation. The latest weak-swirl configuration is a recent discovery which has commercial potential in addition to its significance to fundamental research. These burner configurations are designed to facilitate the comparison with statistical one-dimensional (1-D), deterministic two-dimensional (2-D) models, and three-dimensional (3-D) direct numerical simulations.

Several well-established laser diagnostic techniques with high spatial and temporal resolutions are used to measure statistical moments and correlations of velocity and scalars (i.e., gas density, reaction progress variable). These techniques include laser Doppler anemometry (LDA) for simultaneous measurement of two velocity components and Rayleigh scattering from a focused laser beam for density measurements. We are the pioneer in the development of linear array of Rayleigh scattering and the

applications of LDA to measure conditional velocity statistics and to trace the flowline by auto feedback control. Another scalar diagnostic includes laser-induced Mie scattering from silicone-oil droplets (MSOD) for measuring the reaction progress variable and flame crossing frequencies. Mie scattering is also used for laser sheet imaging of the flame geometry by high-speed tomography.

Typical turbulence intensities we have studied thus far are from 5% to 10%. The turbulence Reynolds number, Re_l, is in the range of 100. These are the conditions which generate the so-called wrinkled laminar flamelets. The chemical reaction time scales are small compared to those of turbulence, and the flame zone can be treated as consisting of a wrinkled thin reaction zone (i.e., the flamelets) separating regions of cold reactants and hot products. The global turbulent burning rate may be determined in terms of the flame surface geometry and the local burning rate. The local instantaneous burning rate of the sheet is, in turn, dependent on the local strain in the flow and the flame-front curvature. This concept has been successfully employed in a variety of models including the statistical 1-D model by Bray, Moss, and Libby (BML) and 2-D deterministic vortex dynamics model by Chorin.

Flamefront Curvature

At present, it is only possible, by laser sheet tomography, to measure two-dimensional distributions of the flamefront curvature. In order to obtain insight into the three-dimensional structures, these measurements were compared with numerical simulations of passive flame propagation within three-dimensional Navier-Stokes turbulence conducted by Dr. William Ashurst of Sandia National Laboratories (Livermore, California). The experimental configuration used was a premixed methane/air flame stabilized at a stagnation point. Oil droplets seeded into the flow allow imaging of the flame front by a sheet of laser light. The mean progress variable was determined by averaging many flame images, and the flame curvature distribution was obtained as a function of location within the turbulent flame zone. The computed flame geometry and flame strain rate were also obtained as a function of progress variable, and planar slices were taken to provide information
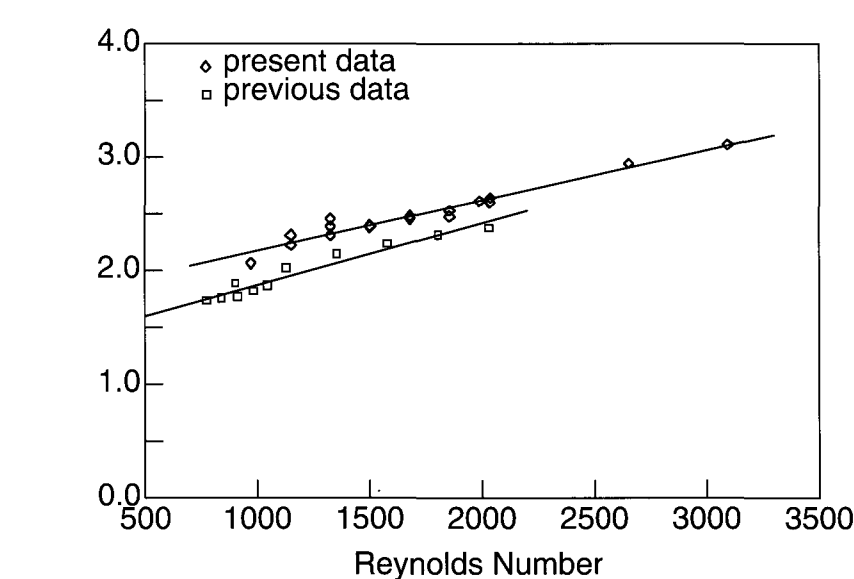

Figure 1. *Reduced flame flickering frequencies $i = v_n/(\tau + 1)$ vs. Re.*

directly comparable to the experimental data. The curvature distributions were determined in each eighth of the progress variable; the simulation results were normalized by the Taylor length; and an effective Taylor length was estimated for the experimental results.

Distributions of curvature as seen in two-dimensional slices exhibit a change with location in the turbulent flame zone. At the front of the flame zone, 78% of the flame front has positive curvature (convex to the reactants) whereas at the back only 40% is positive. The mean positive curvature does not change with location while the mean negative curvature changes linearly with location, the largest magnitude being at the back of the flame zone. The mean curvature as a function of location changes from positive at the leading edge to negative at the trailing edge. From the computed surface eigenvalues, the most probable flame shape is cylindrical, and the computed planar curvature distributions could be matched to the eigenvalue distributions by a scaling obtained from viewing a cylinder at all possible angles. The strain rate in the plane of the flame does not depend upon location, and the distribution is approximately Gaussian. Based on these passive flame dynamics, it appears that experimental planar images may be converted into distributions of three-dimensional flame stretch.

Coupling of Premixed Flames with Buoyancy

As mentioned earlier, premixed tur-

bulent flames are sensitive to conditions in their surroundings. Gravity, therefore, has profound effects on many aspects of the flame propagation including burning rate, stabilization, extinction, and pollutant formation. Our approach to gain a fundamental understanding of the gravitational effects on flame-turbulence interaction processes is to investigate low Reynolds number premixed turbulent flames in normal (+g), reverse (-g), and microgravity (mg). This important turbulent flame propagation problem is not well understood and has yet to be considered in current turbulent combustion theories. Our experimental results are expected to provide guidance and validation for the development of turbulent combustion models to include the effects of gravity. The mg experiments were performed at the 2.2 second drop tower at NASA Lewis Research Center in Cleveland, Ohio. The flame configuration is a small (25 mm diameter) conical Bunsen type flame. This burner uses a ring stabilizer which enables us to stabilize lean conical flames. Laser schlieren coupled with computer-controlled image processing was the primary diagnostics to characterize the behavior of the aerodynamic flowfield and mean flame properties under microgravity. Laboratory experiments of +g and -g flames also include the use of two components laser Doppler anemometry.

The results show that buoyancy-driven instability is found to be the cause of the well-known flame flickering phenomenon. The mechanics is associ-

ated with an unstable interface generated outside of the flame zone between the combustion products and the room air. This interface pulsates at a regular frequency and generates flow fluctuations upstream of both laminar and turbulent flame zones. The flickering frequencies of laminar and turbulent flames are found to scale with the flow Reynolds number and heat release (Fig. 1). Flame flickering ceases to exist in reverse gravity when the flame is turned upside-down (-g) and in microgravity (mg). Another means to characterize the effects of gravity is to compare the flame heights. The -g flames are found to be generally taller than the +g flames. The mg laminar flame heights are between those of +g and -g flames but show a growth trend with Reynolds number more consistent with the +g flames. The turbulent mg flames are shorter than the +g flames. The different trends observed for laminar and turbulent flames in microgravity suggests that turbulent transport is influenced by the surrounding flow field.

Premixed Flames in Intense Turbulence

With increased turbulence intensity, the flamelet concept is no longer valid. It has been postulated that the small turbulence eddies penetrate the flamelets. These small eddies increase turbulence transport and broaden the re-action zone thickness. This is the so-called "distributed reaction zone" regime of premixed turbulent flame. Because of these changes in the reaction zone, the burning rate may not be related to the flame surface geometry. The evolution from flamelets to distributed reaction zone has yet to be validated by experiments. Theoretical treatment of premixed flames with intense turbulence is not well developed.

During 1993, we developed a burner for investigating premixed turbulent flames propagating in intense isotropic turbulence. The burner exploits the large stabilization range provided by the weak-swirl configuration. To produce intense turbulence, we adopted a turbulence generator designed by Videto and Santavicca. This setup produces stable flames propagation under turbulence intensities of up to 20%. The experiments were designed to investigate systematically the changes in flame structures for conditions which can be classified as wrinkled laminar flame, corrugated flames, and flames

with distributed reaction zones. These are the first successful experiments to produce steady (i.e., continuously burning) intense premixed turbulent flames. All previous measurements of flames under similar conditions have used unsteady (i.e., transient) flame propagating within combustion vessels.

Laser Doppler anemometry and Rayleigh scattering techniques were used to determine the turbulence and scalar statistics. Under test intense turbulence conditions, the flames are found to produce very small changes in the mean and rms velocities. The flame-speed is found to increase linearly with turbulent kinetic energy. The most interesting result is that these flame-speeds are much higher that those measured in unsteady flame experiments (Fig. 2). The fundamental difference between steady and unsteady flame propagation may account for the discrepancies. The Rayleigh scattering results were analyzed to obtain the probability density function. The expectation was that, for flames within the distributed reaction zone, the probability of encountering the burning states would be higher. Comparison of the Rayleigh probability density functions for flames within the flamelets regimes and those within distributed reaction zone regime revealed very little differences. These results show that no drastic changes in flame structures occurred. This suggests that the wrinkled flamelets evolve gradually into distributed reaction zones and more sophisticated diagnostics are needed to provide more definitive answers.

Theoretical and Numerical Analysis

All the premixed flame systems which we have studied experimentally propagate through divergent flow fields produced by the flow geometry (the stagnation or weak-swirl flames) or induced by the heat release (Bunsen, or v-shaped flames). It has been customary to idealize these flames as one-dimensional and to estimate the turbulent burning rate by the cold boundary velocity normal to the mean flame position. The assumption of one-dimensionality is not well founded. A study was undertaken to determine the burning rate of non-one-dimensional premixed turbulent flames based on fundamental conservation principles which breaks with the convention of using the cold boundary mass flux. The approach uses direct analytical integration of the balance equation for the mean progress variable, $\bar{c}$. A relationship was derived showing the importance of considering mean velocity gradients and turbulent transport transverse to the mean turbulent flame and also the mean flame shape. A position in the flame zone was identified where the local mass flux normal to the mean flame zone equals the mean rate of creation of products through the turbulent flame. Only at this position can the mass flux be related to a one-dimensional turbulent burning velocity and identified with the mass burning rate. The analysis is valid generally but was applied in detail to stagnation flames because of their relatively simple flow geometry. Under condi-
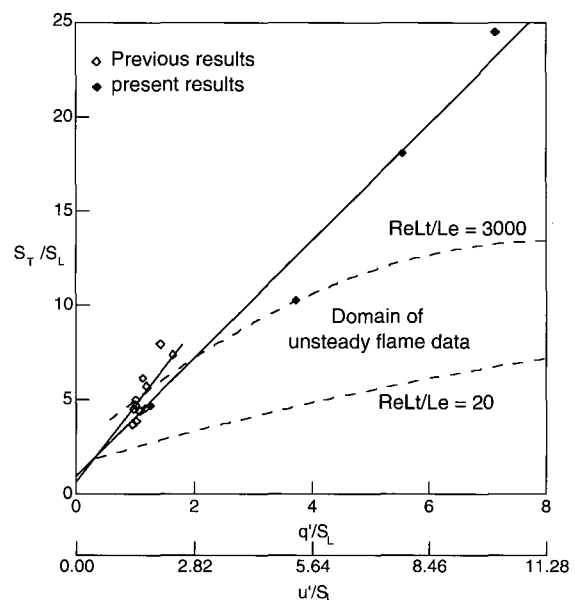

Figure 2. *Correlation of the burning rate ratio and the turbulent/ laminar speed ratio.*

tions of zero turbulent transport transverse to the mean flame orientation, the burning rate of the flame per unit area is the local mass flux weighted by a local gradient in $\bar{c}$ integrated through the flame. Further analysis showed that ignoring nongradient transport leads to an underestimation of the burning rate. Results of a numerical simulation of stagnation flames stabilized in two opposed reactant streams were used to compare the burning rate determined from the above analysis with the value estimated from the cold boundary mass flux. Large differences are observed especially when $\bar{c} \ll 1$ at the stagnation surface.

Our second theoretical study of premixed turbulent flames involves the development of deterministic models of turbulent combustion using Chorin's vortex dynamics method. In contrast to the statistical modeling approach where the changes in flame turbulence are modeled and used as input parameters, the vortex dynamics model is capable of predicting these changes and other flame phenomena, in particular, the flamelet geometry. In simulating the flamelets, one needs to follow the evolution of the flamelets whose speed depends on the local curvature. The algorithms approximate the equations of motion of propagating fronts with curvature-dependent speed which are called PSC schemes for Propagation of Surfaces under Curvature. These algorithms are coupled to a vortex dynamics approach to describe both the turbulence in the oncoming stream and turbulence production by the flame itself and a volume production model to represent combustion heat release. Various statistical data including conditioned and unconditioned mean and RMS values of the two velocity components and the Reynolds stress can be deduced from the numerical results and compared with experimental data.

We have developed a two-dimensional premixed turbulent flame model which focuses on the structure of v-shaped free-burning anchored flames including the effects of advection, volume expansion, flame-generated vorticity, and curvature effects on the laminar flamelet propagation speed. Except for the restriction to two-dimensionality, this model is a fairly complete numerical representation of our previous experimental work under the assumptions inherent in the wrinkled laminar flamelet model

where the flame can be treated as a vanishingly thin interface separating reactants and products. The results obtained thus far are extremely encouraging; they bear a striking resemblance to the tomographic data we have obtained previously on turbulent v-flame structure. The results also show that vorticity production by baroclinicity at the flamefront alters the mean angle of the flame. The thickness of the flame brush due to oscillations produced by the incoming turbulence appears to be consistent with what we observe experimentally. In addition, the numerical results can be analyzed to obtain detailed velocity statistics for direct comparison with our LDA data. These quantities include the vorticity, integral scale, and Reynolds stresses in the burnt gas. We have experimental data on the integral scale and Reynolds stresses with which our numerical results can be compared, and we are in the process of doing this.

Technology Transfer

In addition to its scientific significance, the weak-swirl burner is ripe for technology transfer. The burner has a broad operating range and, in particular, supports stable combustion in very fuel-lean conditions The emission of oxides of nitrogen NO_x from lean flames are very low. The level measured in our laboratory burner operating at 30 kW is less than 10 ppm. This power output is the same as residential air and water heaters. The development of reliable low emission systems based on the weak-swirl burner to replace current models will contribute to the improvement of regional and indoor air quality. A patent is being sought for the weak-swirl burner. We have been awarded a DOE Energy Research Laboratory Technology Transfer project to develop a Cooperative Research And Development Agreement (CRADA) with Teledyne-Laars in Southern California to commercialize the weak-swirl burner for use in small to medium water heaters. Several approaches to implement this new technique will be sought. The major focus is to develop a production prototype of a 14- to 20-kW water heater. Another goal is to design modular burners which can be used to retrofit existing systems. The long-term objective is to scale the system to 140 kW. Because the operating principle is understood, the approach to scaling the

design to different power ratings would be relatively straightforward.

Planned Activities

Work will continue on developing methods and techniques to extract information on the complex three-dimensional flamelet geometry from two-dimensional imaging data. This is accomplished by comparing the experimentally determined values of flame wrinkle scales and curvatures to similar information derived from three-dimensional direct numerical simulations of premixed turbulent flames.

We plan to develop Planar Laser Induced Fluorescence imaging technique to investigate the flame structures of the intense premixed turbulent flames. The results will enable us to infer if the reaction zone thickness is broadened by small-scale turbulence. A series of studies will also be carried out on resolving the difference shown by the flamespeeds of steady and unsteady flames.

The investigation of the flame/gravity coupling will be extended to include conducting microgravity experiments on board NASA Lewis Research Center's Learjet. The parabolic flight experiments provide a much longer reduced gravity periods for data collection. As a bonus, these flights offer enhanced gravity (about 2 g) to study another dimension of flame/gravity coupling.

The development of deterministic vortex dynamic models of premixed turbulent flames will focus on predicting the flame phenomena observed by the experiments. We plan to apply our model to problems of stagnation flow turbulent flames stabilized by a plate or by two opposed streams. Both configurations are axisymmetric and considered to be most suitable for investigating fundamental processes of turbulence-flame interactions.

Work planned for the CRADA developed with Teledyne-Laars will include testing the weak-swirl burner in enclosures and evaluating its operation stability under fuel lean conditions. A demonstration model of a water heater with heat exchanger provided by Teledyne-Laars will be constructed.

Reference

Videto BD, Santavicca DA. *Combustion and Flame* 1991; 76: 159.

Combustion Modeling

J. Garay, J. del Rosario, N.J. Brown

Our research is directed toward building more robust combustion models that can be used as design tools for future generation combustors. These models will help identify combustion characteristics that are important in optimizing the tradeoff between reduced emissions and high energy efficiency. Current modeling efforts are directed toward

- adding chemistry, described by a comprehensive chemical mechanism, to models of turbulent reacting flows;
- modeling NO and CO chemistry in premixed and partially mixed laminar flames burning natural gas; and
- optimizing schemes for pollutant reduction.

In collaboration with colleagues at Sandia National Laboratory and the University of California, Berkeley, we have developed a new user-friendly toolkit for parallel computing to enable us to perform the first calculation of NO production in a turbulent reacting jet using a *comprehensive* chemical mechanism. The net production of NO was calculated for 40% He + 60% H_2-air turbulent non-premixed flames for several Reynolds numbers. The comprehensive mechanism consists of 10 species whose chemistry is described by 13 reactions. Incorporating a comprehensive chemical mechanism into a model describing turbulent reacting flow would not have been possible without parallel computing. A calculation of this type on a single state-of-the-art workstation would take upwards of 50 days and on a single dedicated supercomputer on the order of five days. The jet flame was modeled with a probability density function (PDF) code. Calculations were also performed with a reduced mechanism consisting of two global reactions. The reduced mechanism was derived from the comprehensive mechanism by assuming partial equilibrium for the radical species. Thermal NO formation and its dependence on Reynolds number calculated with the comprehensive mechanism are in excellent agreement with experiments of Driscoll et al. (Figure). Large deviations from equilibrium theory were observed, and less satisfactory agreement was found between the experimental NO con-

centrations and values calculated using the reduced mechanism. These results emphasize the importance of incor-porating more comprehensive chemistry into models to describe flames that deviate substantially from equilibrium. We are augmenting the toolkit to incorporate other reacting flow models to allow combustion scientists to access the power of parallel computing to treat other combustion problems requiring a more robust chemical description. Future plans also include modeling flames of different compositions and different chemical mechanisms.

We have modeled highly strained premixed laminar flames in the presence of a heat-transfer surface. We developed a very good "guess" algorithm and used a combination of adaptive and fixed gridding to achieve highly precise, computer-intensive converged solutions. Solutions were obtained as a function of the following parameters: equivalence ratio, disc temperature, and disc separation. We determined the effect of the disc by examining computed temperature, velocity, and species profiles and by comparing strained flame properties at the location of the disc (1.0 or 2.0 cm) with those of a premixed laminar flame (nonstrained flame) at the same axial location. The presence of the disc has a threefold effect. First, because the velocity is zero at the disc, the reaction time associated with the flame in the presence of the disc is longer. Second, by fixing the plate temperature at a value different from the nonstrained

flame, the temperature profile between the burner surface and flame has a very different shape. Unless the disc temperature is close to the nonstrained value, the maximum temperature of the nonstrained flame is usually higher. The third effect is that the disc acts as a catalyst. For a disc separation of 1.0 or 2.0 cm as the disc temperature was decreased from its nonstrained value to 500° K, the HO_2 and CO_2 concentrations at the disc increased and the O, OH, NO, and CO concentrations decreased. An optimum burner insert/flame combination for reducing pollutant emissions would have the coldest surface located as close to the burner as possible for a stable flame to be maintained.

Common to all our modeling efforts is mechanism development and mechanism reduction. We have compared our large comprehensive mechanism for methane/air with the experimental measurements of Bartok et al. The comparison was very satisfactory. Because the mechanism is so complex, we are currently using advanced sensitivity analysis techniques—namely, principal component analysis—to reduce it. We have determined reduced mechanisms that can model NO and CO chemistry in flames, perfectly stirred reactors, and plug flow reactors. We have also developed mechanisms that are suitable for generating the temperature profile of combustion systems. The latter is very important in building solutions requiring the solution of the energy equation.

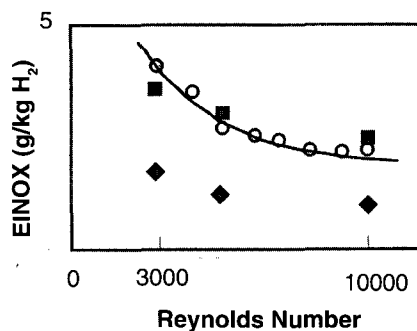**Figure.** *Plot comparing calculated EINOX (total grams NO_x/kg fuel) versus Reynolds number with the experimental values of Driscoll et al.*

○ experiment (Driscoll, Chen, Yoon, *Combustion & Flame* 1992; 88: 37.
■ calculation
◆ reduced mechanism

We have completed our study of the selective reduction of NO by $HNCO_5$ and have initiated new research on a staged combustion technique for NO reduction called reburning. We are determining optimum conditions for each of the three or more stages that result in the optimum reduction of NO and the minimum emission of CO.

We have begun to model a Bunsen burner-type flame that is commonly used by the gas industry in home appliances. Experiments are being performed on this flame at UCB, and intercomparison between our computed and their experimental results on CO will be used to validate the hydrocarbon portion of our mechanism. We will approximate the system as being a parabolic set of equations by ignoring axial diffusion. Combustion along the radial direction will be treated as a two-point boundary value problem, and along the axial direction, it will be treated with plug flow. This approximation causes an error of approximately 20% in the calculated NO profiles. Solving the problem as a full set of elliptic equations has an enormous computational burden associated with it. *The elliptic problem requires approximately 300 hours of Cray computer time for a single flame.* We will use parallel processing to solve the elliptic problem with the parabolic solutions as initial guesses for the elliptic solutions.

References

Koszykowski ML, Armstrong RC, Cline Jr, RE, Macfarlane JF, Chen JY, Brown NJ. "ACME—The Advanced Combustion Modeling Environment." In: *Computing at the Leading Edge: Research in the Energy Sciences.* U.S. Government Printing Office Pub. No. 1993-785-007, p. 61, 1993.

Koszykowski ML, Armstrong RC, Chen JY, Dai F, Brown NJ. Turbulent jet flame modeling with comprehensive chemical kinetics for NO_x prediction. Submitted to *25th Symposium (International) on Combustion.*

Driscoll JF, Chen RH, Yoon Y. *Combust. Flame,* 1992; 88: 37.

Bartok W, Engleman VS, Goldstein R, Del Valle EG. *AIChE Symp.* 1972; 68: 30.

Brown NJ and Garay J. Modeling and sensitivity analysis studies of the reduction of NO_x by HNCO. Submitted to *Combustion Science and Technology.*

Combustion Chemistry

J. Chang, N.J. Brown

Combustion modeling is a broad endeavor that can begin with the calculation of potential energy surfaces and involve intermediate stages (e.g., calculation of state-to-state cross sections) that are averaged to yield thermal rate coefficients. The thermal rate coefficients are then used in a combustion model which includes both a chemical and fluid mechanical description to predict bulk quantities of interest to combustion—e.g., concentrations, temperature, pressure, and heat release. In a flowchart (Figure) showing the hierarchical connection between microscopic and macroscopic variables at different levels of combustion modeling, each box corresponds to a theoretical construct or model that can be used to calculate observables or dependent variables from model input parameters. Each of the intermediate model outputs can in turn be regarded as model inputs to a higher or more macroscopic level of theory. Our research is concerned with the development and use of sensitivity analysis tools to probe the response of dependent variables to variations in model input parameters. Sensitivity analysis is important at all levels of combustion modeling.

In the past six years, there have been several dramatic advances in both experimental and theoretical capabilities to describe chemical reactions at the fundamental level of quantum mechanical reactive scattering. Our research in this area continues to be focused on elucidating the interrelationship between features in the underlying potential energy surface (PES) obtained from *ab initio* quantum chemistry calculations and their responses in the quantum dynamics, e.g., reactive transition probabilities, cross sections, and thermal rate coefficients. The goals of this research are: 1) to provide feedback information to quantum chemists in their PES refinement efforts and 2) to gain a better understanding of how different regions of the PES influence the dynamics. These investigations are carried out with the methodology of quantum functional sensitivity analysis (QFSA).

Our effort in this area has evolved from a series of one-dimensional studies on the collinear H + H_2 exchange reaction where the H-atom and the H_2 molecule are constrained to lie on a straight line. This past year, we concluded the first QFSA study of the H + H_2 reaction in three dimensions (3-D), that is, without imposing any artificial dimensionality constraints. We also developed another program for calculating sensitivities that is capable of handling additional complexities involved in a general atom-diatom reaction. This program will be used in a sensitivity analysis study to deter-
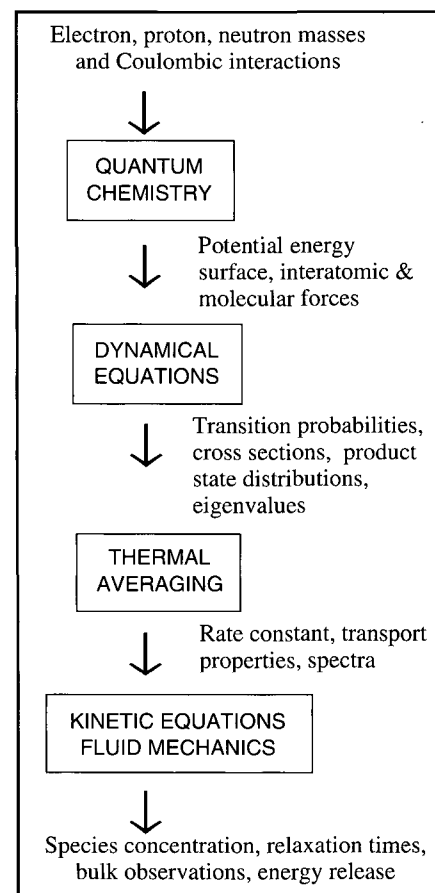
Figure 1. *Flowchart illustrating the hierarchical connection between microscopic and macroscopic variables at different levels of combustion modeling.*

Electron, proton, neutron masses
and Coulombic interactions

↓

QUANTUM
CHEMISTRY

↓ Potential energy surface, interatomic & molecular forces

DYNAMICAL
EQUATIONS

↓ Transition probabilities, cross sections, product state distributions, eigenvalues

THERMAL
AVERAGING

↓ Rate constant, transport properties, spectra

KINETIC EQUATIONS
FLUID MECHANICS

↓

Species concentration, relaxation times, bulk observations, energy release

mine how different isotopic analogs of the H + H_2 reaction sample the potential energy surface. These investigations are important because the H_3 system plays an important role in developing theories of chemical reactivity.

Another tool developed this past year aids in the visualization of sensitivities. It is an image creation and processing software built from Silicon Graphics Explorer modules. This software enables us to view the evolution of sensitivity structure at sequential energy slices in a continuous fashion. The images are color coded to designate regions of large sensitivity and were saved onto an optical laserdisk for making movies. Below are some of the results gleaned from our first 3-D study of the H + H_2 reaction where the collisions are restricted to zero total angular momentum.

Figure 2 shows two energy slices of the reaction probability sensitivity starting from an initial vibrational (v) and rotational (j) state v = 0, j = 0 to a final rovibrational state v′ = 0, j′ = 0. At the lower energies (Fig. 2a), there is a close resemblance between the 3-D and the collinear sensitivities. There is a large region of negative sensitivity near the saddle point of the PES followed by oscillatory behavior toward the asymptotes. With increasing energy, the positive shoulders grow, become more prominent, and move toward the barrier top where they coalesce in the inner corner (tunneling) region of the PES and eventually displace the negative sensitivities at the barrier top. Unlike the collinear sensitivities, the magnitudes of these 3-D sensitivities are relatively small compared to those at higher energies At even higher energies, the pattern seen at lower energies repeats itself. The sensitivities at the shoulders grow in magnitude and move toward each other eventually coalescing at the inner corner of the PES. Each time the shoulders coalesce though, they cut further into the inner corner. In the meantime, the sensitivities near the barrier top decrease in magnitude. The result is that the extremes of the sensitivity peaks trace out a path that is significantly removed from the reaction path (Fig. 2b). In fact, the region of the PES followed by the reaction path across the barrier is important only for a small energy regime just beyond the threshold energies.

For the cumulative transition probability sensitivities (obtained by summing the individual state-to-state transition probability sensitivities from v = 0, j = 0 to all the open product channels), the regions of large sensitivities are localized in the neighborhood of the potential barrier for low collision energies. However, with increasing energy, the positive sensitivity on the barrier shoulder on the reactant side grows in prominence, moves toward the barrier top, and eventually displaces the negative sensitivity at the transition state.

From about 0.75 eV (total energy) to 0.98 eV, the sensitivities at the top of the barrier are positive, which implies that an increase in barrier height actually increases reactivity (with corresponding decreases in nonreactive transitions). At higher energies, changing the barrier height has negligible effect on reactivity as the regions of large sensitivity follow a path that "cuts the corner" and is far removed from the reaction path, in agreement with observations made on the (v = 0, j = 0) to (v′,j′) = (0,0) and (0,1) transition sensitivities. These

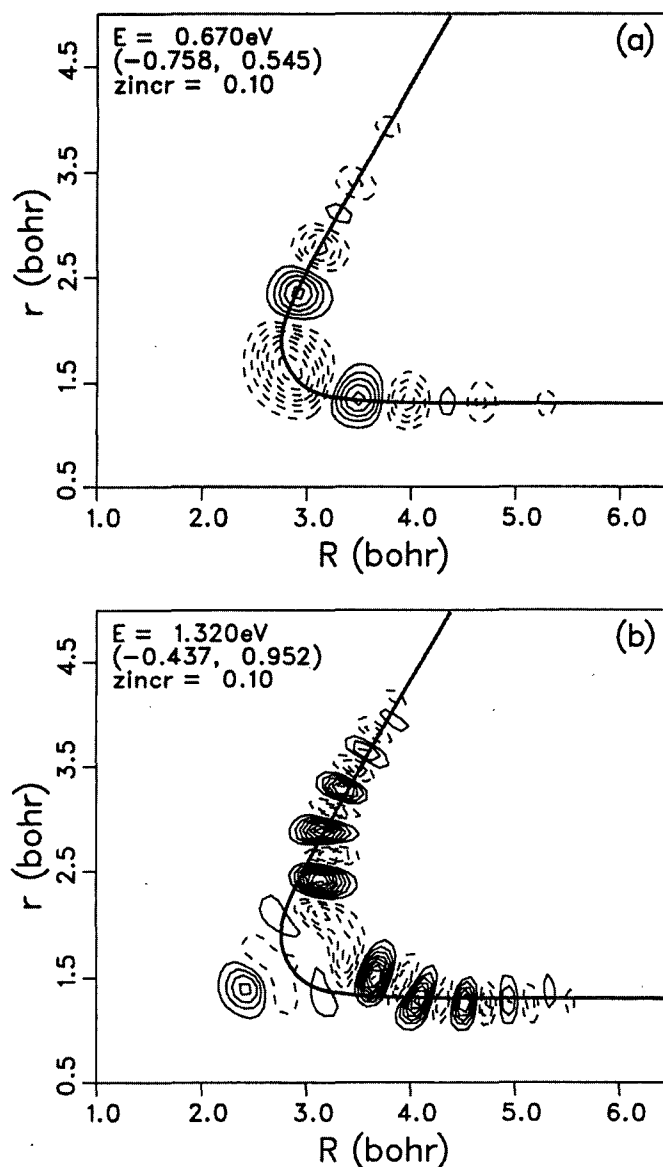**Figure 2.** *Sensitivity maps for the v = 0, j = 0 → v′= 0, j′= 0 transition probability at two energies (a) E = 0.67 eV and (b) E = 1.32 eV and at a scattering angle of 180°. The contour values are drawn in increments of zincr shown on the plots. Positive contours are represented by solid lines and negative contours by dashed lines. The zero contour line is omitted. The numbers in parentheses represent the minimum and maximum sensitivity values on an 80 × 65 rectangular grid. All sensitivity contour values are given in units of $eV^{-1}bohr^{-6}$. The reaction path is shown on the plots by a solid heavy line.*

results further attest to the fact that the potential-to-dynamics interrelationship is far richer and more complex than the well-known simple notions concerning how changes in barrier height and barrier width affect chemical reactivity.

Among the other regions of high sensitivity found in our study, the most notable is the outer corner of the PES for bent geometries. This is the region where the H_3 molecular conformation is more compact than the conformation at the barrier top. The sensitivity magnitudes tend to decay as the geometry becomes more bent, but the sensitivities at the outer corner region tend to decay slower with scattering angle and may, in fact, increase for some noncollinear geometries before they decay.

In 1994, we shall perform sensitivity

studies on the $D + H_2$ and $H + D_2$ reactions (both of which share the same underlying PES as the H_3 system) to see how and whether or not these isotopic reactions provide information about different regions of the PES. We shall perform total integral cross-section sensitivity analyses which involve summing sensitivity contributions from several total angular momentum. We shall also begin to analyze the sensitivity structure for the $F + H_2$ and $H + O_2$ reactions. The latter is one of the most important chemical reactions in combustion, and new global potential energy surfaces for both these two reactions are soon becoming available.

References

Chang J, Brown NJ, D'Mello M, Wyatt RE, Rabitz H. Quantum functional sensitivity analysis for the collinear H+ H_2 reaction rate coefficient. *J. Chem. Phys.* 1992; 96: 3523.

Chang J, Brown NJ, D'Mello M, Wyatt RE, Rabitz H. Quantum functional sensitivity analysis within the log-derivative Kohn variational method for reactive scattering. *J. Chem. Phys.* 1992; 97: 6226.

Chang J, Brown NJ, D'Mello M, Wyatt RE, Rabitz H. Predicting observables on different potential energy surfaces using feature sensitivity analysis: Application to the collinear H + H_2 exchange reaction. *J. Chem. Phys.* 1992; 97:, 6240.

Chang J, Brown NJ. Quantum functional sensitivity analysis for the 3-D (J = 0) H + H_2 reaction. *Int. J. Quantum Chem.* 1993; 27, 567.

Atmospheric Aerosol Research

Contribution of Sulfate and Organic Aerosol to Cloud Condensation Nuclei at a Marine Site

T. Novakov, C. Rivera-Carpio, J.E. Penner*, C.F. Rogers†

Modeling studies show that anthropogenic aerosols, due to their light scattering properties and their ability to serve as cloud condensation nuclei (CCN), may cause a globally averaged climate forcing comparable in magnitude but opposite in sign to the forcing due to "greenhouse" gases, thereby masking, to some extent, the effect of greenhouse gases. The backscattering of solar radiation by anthropogenic aerosols tends to cool the atmosphere. In addition, increasing concentrations of anthropogenic aerosols may contribute significantly to cloud condensation nuclei (CCN) concentrations, which results in increasing albedos of clouds and thus further contributing to atmospheric cooling. The relevant anthropogenic aerosol is composed of varying amounts of chemical species, mainly sulfates (from SO_2), organic particles (from gas-to-particle conversion of reactive hydrocarbon precursors, and primary organic

*Lawrence Livermore National Laboratory
†Desert Research Institute, Reno, NV

aerosol from combustion processes), elemental or black carbon (from incomplete combustion), ammonium (from biological sources), and some nitrate. Of these, sulfate aerosol received most attention because of the relatively well documented global distribution, and the known optical and nucleation properties of this aerosol. In contrast, the data on the concentrations, sources, and properties of other major components of anthropogenic aerosols are much scarcer. This is particularly true for the organic aerosol species because most systematic aerosol measurements have emphasized inorganic constituents. Obtaining such data is important because the optical and nucleating properties of anthropogenic aerosols depend on the size and chemical composition of all relevant species.

As part of our ongoing project on the modification of cloud optical properties by aerosols, we have been engaged in aerosol and cloud microphysical measurements on El Yunque peak (18°19'N,

65°45'W; elevation ≈1,000 m), located on the eastern end of Puerto Rico. Our results obtained previously at this site have shown that CCN concentrations cannot be explained by sulfate concentrations alone. We have therefore performed measurements and data analyses with the objective to quantify the contributions of sulfate, seasalt, and organic aerosol mass concentrations to the CCN number concentrations.

The following results were obtained in March/April 1992:

- The impactor-derived mass size distributions of aerosol sulfur, chlorine, and organic carbon (OC). (The impactor—Microorifice Uniform Deposit Impactor—was on loan from the Desert Research Institute, Reno, Nevada, where the chemical analyses of the impactor samples were performed);
- CN concentrations;
- CCN concentrations measured at 0.5% supersaturation; and
- total nonseasalt (nss) sulfate mass

concentrations determined concurrently with CN and CCN measurements.

The approach was to convert the measured mass size distributions to number size distributions of sulfate, seasalt, and organic aerosol from which the contributions of these species to the CCN and total aerosol number concentrations could be estimated.

The data obtained demonstrate that most of the NaCl (or seasalt) mass is associated with large particles; the aerosol sulfur mass is confined to a relatively narrow range of smaller particles; and the OC size distribution is more evenly spread over the entire size range extending to the lowest size cuts, with a small fraction associated with the supermicron particles. Converting the mass size to number size distributions shows that organic aerosols contribute significantly more than sulfate aerosols to the number concentrations of small particles, despite the fact that the total sulfate mass concentrations were generally higher than OC. Because the Cl mass concentrations were below detection in small size impactor stages, the number concentrations of the seasalt aerosol were found to be insignificant.

We have used the sulfate and organic aerosol number concentrations to estimate two sets of aerosol number concentrations N_{tot} and $N_{0.025}$. N_{tot} refers to the total number concentrations, obtained by integration of the number size distributions from $r_{min} = 0.015$ to $r_{max} = 3.00$ μm. The r_{min} value of 0.015 μm chosen corresponds to the radius of particles counted with an efficiency of >50% by the aerosol counter used in the experiment. $N_{0.025}$ refers to the number concentration of particles with radii $r_{min} > 0.025$ μm. Ammonium sulfate particles in this size range are expected to be activated at 0.5% supersaturation and therefore counted as CCN. These derived quantities were compared with clear-air total aerosol and CCN (at 0.5% supersaturation) concentrations measured throughout the duration of the experiment. The comparison of the data shows that the average measured CCN concentration of 556 cm^{-3} is in remarkably good agreement with the sum of 578 cm^{-3} of average estimated concentrations of $N_{0.025}$ (Sulfate) and $N_{0.025}$ (Organic). The mean measured CN concentration of 2322 cm^{-3} is comparable to the sum N_{tot} (Sulfate) and N_{tot} (Organic) of 1778 cm^{-3}. These

results indicate that at this marine site about 37% of the CCN number concentrations can be accounted for by sulfate and 63% by the organic aerosol mass concentration.

These conclusions, if confirmed at other locations, may be of particular relevance to the question of CCN-cloud droplet relationship because theoretical studies have shown that the production of new sulfate CCN is not the major pathway for the conversion of anthropogenic SO$_2$ emissions to SO$_4^{2-}$. Anthropogenic sulfate mass is believed to be principally produced by SO$_2$ oxidation in cloud droplets. This formation pathway would not produce new sulfate CCN, only larger particles formed on preexisting aerosols. In contrast, the formation of organic aerosol does not involve aqueous chemistry. It is derived either from direct emissions of primary particles, or produced by condensation of low vapor pressure products of gas-phase reactions of reactive hydrocarbons. Therefore, it can be expected that the number concentration of organic aerosol, including the fraction that serves as CCN, should be more strongly related to the emissions of anthropogenic pollutants.

Ecological Systems

Genetic Ecotoxicology

S. Anderson, J. Harte, W. Sadinski, E. Gray, G. Wild, J. Hoffman, E. Hoffman, D. Steichen, J. Jelinski

The broad goal of our project is to improve the application of genetic toxicology in ecological risk assessment. Our particular interest is in evaluating relationships between reproductive effects, genotoxic effects, and fitness parameters in varied species. We are also concerned with the broad application of genotoxicity and reproductive test techniques to the evaluation of effects in complex media such as soil and sediment. Toward that end, we have completed work on three specific goals:

• to determine the utility of a nematode *Caenorhabditis elegans* bioassay in evaluating genotoxic and repro-

ductive effects in contaminated soil and sediment with special emphasis on effects of arsenic;

• to evaluate the ecological consequences of multigeneration exposures to genotoxic substances using the nematode *C. elegans;* and

• to evaluate whether selected life history characteristics confer vulnerability to genotoxic substances.

Assessing potentially toxic effects of sediment and soil contamination is an important goal in ecotoxicology. Few tests exist to assess the sublethal effects of sediment contamination, and none can reliably assess effects in both contaminated soil and sediment.

There are numerous instances in which tens of thousands of cubic yards of contaminated sediments are transferred upland for hazardous waste disposal or for site alterations such as levee maintenance. Currently, techniques are needed to determine whether contaminated sediments are benign or have the potential to cause environmental harm in order to direct decisions regarding appropriate disposal and remediation alternatives.

We have conducted studies to determine the utility of a *C. elegans* assay for evaluating effects of contaminants in sediment pore water. Pore water is the interstitial water between sediment

grains, and it is believed to be a good approximation of the exposures to which infaunal species are subject. Pore water is prepared by centrifuging sediment cores. The supernatant is used for toxicity testing. Our preliminary studies have shown that a one-generation reproductive assay may be an easy and practical technique for assessing sediment contamination. The test will detect effects such as lethal mutations and other factors that affect fertility. Definitive mutagenesis assays may also be conducted in pore water as a higher-tiered alternative. Our recent research has established the test technique for sediment pore water; in subsequent studies, applications to soil will be assessed.

The dose response characteristics of the pore water assay have been established for three metals spiked into both a control buffer and sediment pore water. For arsenate, arsenite, nickel, and cadmium, the Lowest Observed Effect Concentrations (LOEC) were 4.5, 2.5, 0.05, and 0.25 ppm respectively. Using nickel, we also compared the sensitivity of this assay to that of two pore water tests currently used in environmental management. The nematode assay was more sensitive than the other two tests.

Evaluations of multigenerational effects of environmental pollution are urgently needed. Genotoxic chemicals can cause DNA damage which is transmitted from one generation to the next, yet there have been no assessments in genetic ecotoxicology of potential multigeneration effects.

We have assessed brood size and sterility in multigeneration exposures of the nematode *C. elegans* to ultraviolet-B (UV-B) and ethyl methane sulfonate (EMS). In the UV-B experiments, nematodes were subjected to 15 generations of continuous UV-B exposure. For both controls and experimentals, we maintained 12 replicate culture lines. Broodsize was assessed in the progeny of exposed animals, and in each generation, the number of replicates producing completely sterile progeny were assessed. For brood size, a marked initial decline was noted, and this approximately 50% decrease was maintained in every subsequent generation. Thus, multigeneration exposure did not appear to worsen the broodsize effect. In contrast, the number of replicates that were producing sterile progeny followed an unusual pattern of multigenerational effect.

For six generations, there were no replicates producing sterile progeny. Following the sixth generation, there was a steep linear increase in the number of replicates producing sterile progeny. At 15 generations, the experiment was terminated because only three of the original 12 replicates were producing viable progeny. In contrast, all 12 control replicates produced viable progeny for 15 generations.

To determine whether chemical mutagens may also produce multigeneration effects detected as frequency of sterility, we redesigned the experiments emphasizing sterility rather than brood size as an endpoint. In these complex experiments, 25 cultures were maintained for each of five replicates. Nematodes were exposed in batch for four hours every generation during a developmental stage in which primary oocytes and mature sperm have been formed. Frequency of steriles per replicate was calculated by dividing the number of sterile cultures per replicate by 25 (the number of cultures maintained per replicate). These per-replicate frequencies were then averaged and divided by five (the total number of replicates) to obtain treatment means. Progeny of animals exposed for one and two generations elicited mean frequencies of steriles of 0.0 and 0.8 × 10^{-2}, respectively. In contrast, progeny of animals exposed for three and four generations produced frequencies of steriles of 14.8 × 10^{-2} and 25.8 × 10^{-2}, respectively. In four

successive generations, progeny of control animals elicited sterile frequencies of 0.0, 1.6, 0.8, and 1.6 × 10^{-2}. These data show (Figure) that multigenerational effects are clearly discernible and that the frequency of sterile mutants may be an excellent marker for such effects. Patterns of sterility are not predictable, and these vary among genotoxic agents. Dr. David Littlejohn of the LBL Flue-Gas Chemistry Group collaborated on this project.

We completed two studies which explored the significance of genotoxic effects in ecosystems and evaluated aspects of life history traits and ecological parameters that may confer vulnerability. In the first project, we used *Xenopus laevis* tadpoles to evaluate relationships between DNA adducts, micronucleus induction, and time to metamorphosis of tadpoles. The latter is a significant ecological parameter because if tadpoles metamorphose slowly, they would be unable to survive when the ephemeral ponds that they live in dry up. We found positive correlations between DNA adducts, micronucleus induction, and increased time to metamorphosis after 16-day exposures of tadpoles to 7.5-62.5 mg/L benzo(a)pyrene. DNA adducts were analyzed in the laboratory of Dr. Bill Bodell at the University of California, San Francisco. We believe this study is the first example in ecotoxicology of linkages between DNA adducts, micronucleus formation, and a fitness para-
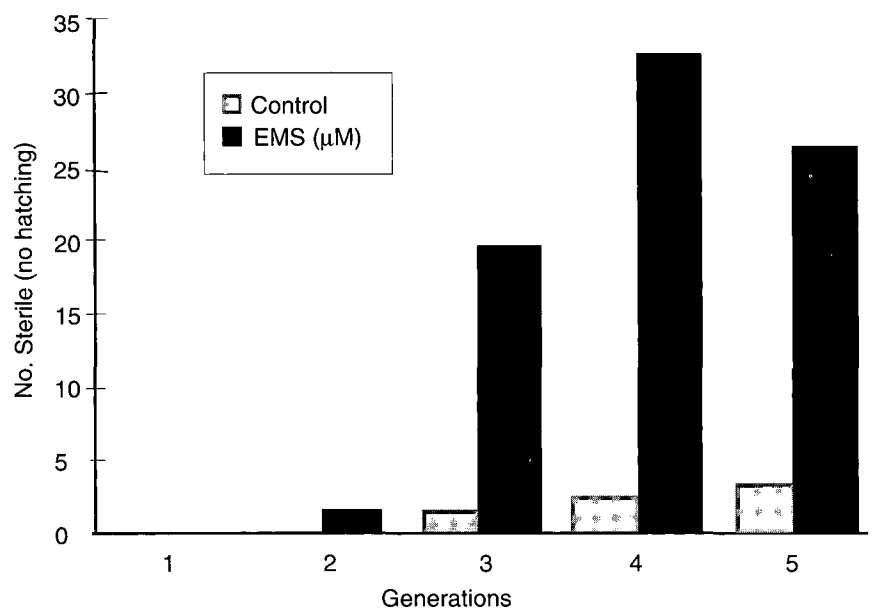

Figure. *Brood size and sterility in multigenerational exposures of the nematode* C. elegans *to ethyl methane sulfonate.*

meter affecting survival and reproductive success. This work is, therefore, a unique example of the potential significance of genotoxic responses in ecosystems.

In the second project, we evaluated, for the first time, female germ-cell mutagenesis in the Japanese medaka *Oryzias latipes*. Previous studies using this fish had evaluated only dominant and recessive lethal mutations in males. We are developing this important animal model to accommodate female exposures because these are more representative of conditions in the environment—animals would typically be exposed as pairs. This will permit further studies of the influence of life history traits on susceptibility to the effects of genotoxic compounds.

In a previous progress report, we described the validation of a sea-urchin anaphase aberration assay that can be widely applied to marine environmental studies. Significantly, this technique was recently adapted to an Antarctic sea urchin *(Sterechinus neumayeri)*, and together with the research team of Dr. Deneb Karentz, we evaluated effects of ambient UV-B in Antarctica on chromosomal damage in these embryos. This work represents the development of the first animal model to evaluate the effects of Antarctic ozone depletion.

During October 1993, we worked with the UC Berkeley Superfund Program to host the "Napa Conference on Genetic and Molecular Ecotoxicology." The goals of the conference were threefold. The first goal was to highlight the state of the art of genetic ecotoxicology. The second

goal was to explore linkages between genetic ecotoxicology and ecological genetics, and the third goal was to improve the implementation of molecular techniques in genetic ecotoxicology. Forty people assembled from around the world, and a framework for research in the coming decades was developed. The proceedings of the conference and the research framework will be published as 25 papers in a dedicated issue of *Environmental Health Perspectives*.

In the coming year, we plan to proceed with four types of studies. First, we plan to evaluate arsenic effects in the other genotoxicity assays described above. These include the medaka dominant lethal test, the tadpole micronucleus test, and a nematode multigeneration effects experiment. The eventual goal of our work is to characterize the effects of arsenate and arsenite in varied ecotoxicological test systems in addition to performing studies of arsenic effects in pit lakes created by mining activity.

Our second goal is to initiate a study using the sea-urchin anaphase aberration assay that has been widely used in our laboratory. The goal of this study will be to determine what developmental stages of the urchin are most vulnerable to the effects of genotoxic chemicals. Currently, we are evaluating whether the effects of arsenate will be manifested in a stage-specific manner using pulsed exposure experiments. This research is being conducted in collaboration with Dr. Gary Cherr and Dr. Gayle Garman at the University of California Bodega Marine Laboratory. Studies using the

sea urchin model to evaluate effects of ozone depletion will also be conducted pending availability of funds.

We also will be conducting studies to develop improved sediment bioassay test techniques for San Francisco Bay. This work will focus on the development of techniques for testing sediment pore water and is being conducted in collaboration with Dr. John Knezovich at Lawrence Livermore National Laboratory.

References

Anderson SL, Hose J, Knezovich J. Genotoxic and developmental effects in sea urchins are sensitive indicators of effects of genotoxic chemicals. *Environmental Toxicology and Chemistry* (in press, 1993)

Anderson SL, Hoffman J, Wild G, Bosch I, Karentz D. Cytogenetic, cellular and developmental responses in Antarctic sea urchins (*Sterechinus neumayeri*) following laboratory UV-B and ambient solar radiation exposures. *Antarctic Journal.* (in press, 1993)

Anderson SL. "Ecotoxicology: Management and science." In: R. Socolow (Ed.), *Industrial Ecology.* Cambridge University Press. (in press, 1993)

Anderson SL. Experimental models linking genotoxic responses and reproductive effects in ecosystems. *Environmental Health Perspectives* (in press, 1993)

Anderson SL, Shugart P, Ford BT, Stegeman J, Wogan G, Hose J, Wirgin I, Suk W. Genetic and molecular ecotoxicology: A framework for the future. *Environmental Health Perspectives* (in press, 1993)

Heavy-Metal Toxicology and Bioremediation

R.J. Mehlhorn, J. Cato, Y.-R. Wu

Many heavy metals are toxic to plants and animals; indeed, heavy metals often accumulate in food chains and pose their greatest threat to predators at the top of these chains. Because of their industrial importance, heavy metals contaminate many areas of the world and threaten the health and safety of human communities and the integrity of ecosystems. Moreover, highly toxic heavy metals like mercury tend to be associated with organic matter (i.e., fossil fuels) and are re-

leased into the environment when the organic matter decomposes or burns.

Prevention and mitigation of heavy metal accumulation in the biosphere poses one of the great challenges of this and future generations. Biological heavy metal control and remediation in conjunction with physical and chemical removal processes may be the most economical and effective approach for restoring and maintaining acceptable heavy metal levels in the environment.

An understanding of heavy-metal toxicity is a prerequisite for regulating human activities that may affect the release of metals into the environment. Among the important toxicity mechanisms of heavy metals is their participation in free-radical processes. Free radicals—that is, reactive molecules containing unpaired electrons—are implicated in the effects of many environmental risks factors such as cigarette smoke. Improvements in detecting "fingerprints" of free radical

damage could lead to more meaningful and efficient analyses of pollutant risks. Free radicals are also produced as an unavoidable consequence of aerobic metabolism in both animals and plants. The "free radical theory of aging" postulates that endogenously produced free radicals are responsible for the eventual deterioration of all higher organisms. Heavy-metal-catalyzed reactions may be a major source of chronic free-radical damage, and an improved understanding of such reactions may offer benefits not only for the abatement pollutant exposure risk but also may lead to an understanding of "normal" deteriorative processes in biological systems and possible interventions in the adverse effects of human aging.

We study biological free-radical damage mechanisms particularly with reference to heavy metals and metalloproteins and possible interventions that may protect against free-radical damage including environmental management to minimize the occurrence of free radical-mediated risks in the biosphere. One component of our research program is the development of improved assays (biomarkers) of free-radical damage. Of particular interest is the role of free radicals in the adverse effects of cigarette-smoke exposure. The reactions of cigarette smoke with blood are being studied in human blood (which is readily available), thus facilitating laboratory studies and the development and implementation of risk-exposure assays.

Another component of our project concerns the development of technologies to remove heavy metals from contaminated environments. We are developing biomass derived from microalgae as well as metabolically active bacteria for the purpose of removing and, possibly, recovering heavy metals from water and soil.

Our principal experimental approach is electron spin resonance (ESR), a highly specific method that detects the magnetic moments of free radicals. The sensitivity of the ESR method is increased substantially by working with "free radical traps" including a number of traps developed in our own laboratory which accumulate ESR-detectable products and which serve to "fingerprint" specific free radicals. The ESR assays are being developed largely in the human red blood cell (erythrocyte). Many air pollutants

readily pass across the lining of the lung and can react with blood components. Such pollutants can be investigated with freshly drawn human blood, thereby avoiding many of the problems associated with animal research.

Another promising bioassay that has been developed during the past year is a scheme for detecting hexavalent chromium in suspensions of living cells. Our new chromate assay specifically detects organic complexes of pentavalent chromium and allows us to study the mechanism of hexavalent chromium reduction in metabolically active bacterial cell suspensions.

We are continuing to conduct biomass manipulations to modify, stabilize, and immobilize algal biopolymers which seek to improve the selective removal of heavy metals from contaminated waste waters and the stripping of the bound heavy metals to generate recyclable biofilters suitable for remediation of toxic heavy metals. Recently we demonstrated that these biofilters bind a variety of organic and metallized dyes used by the textile industry. This has set the stage for our participation in the AMTEX initiative, a partnership of the American textile industry and the U.S. Department of Energy. The AMTEX objective is to develop and implement new technologies for increasing the competitiveness of the U.S. textile industry.

Our recent experiments have helped us to better understand how exposure to cigarette smoke leads to cardiovascular disease and cancer. We demonstrated that exposure of blood to cigarette smoke promotes free-radical formation by hemoglobin products including methemoglobin. In analyzing hemoglobin oxidation products, we identified new markers of oxidant damage in blood. We showed that chelatable iron, an indicator of hemoglobin destruction, can be detected outside of erythrocytes after exposure of blood to gas-phase cigarette smoke. Chelatable iron was also detectable in cigarette-smoke-treated hemolysates. However, we observed that cigarette smoke oxidants released very little iron from hemoglobin in red cells and that iron release from hemoglobin by leukocyte oxidants (e.g., hydrogen peroxide) may be more significant. A major effect of gas-phase cigarette smoke was a depletion of intracellular ascorbate (vitamin C).

The mechanism of this depletion appears to be more complex than simple oxida-tion of ascorbate by gas-phase free radicals. Tar-phase cigarette smoke, on the other hand, exerted its major effect by catalyzing free radical reactions of peroxidases and methemoglobin. During some of these free-radical reactions, cigarette tar components are chemically altered, and our tissue culture data suggest that these altered cigarette tar constituents are more cytotoxic than unmodified tar.

Our work on protein damage focused largely on assay development, a focus that was prompted by the elusiveness of the free-radical effects we sought to resolve. A significant development was a novel free-radical assay that is considerably more sensitive to chronic insult than is the previous method of choice (ESR spin trapping). The new assay, based on mass spectrometry of spin-trap adducts of hemoglobin, demonstrated that hemoglobin was not appreciably oxidized to protein free radicals when ascorbate-depleted blood was exposed to gas-phase cigarette smoke under conditions that caused substantial carboxyhemoglobin formation. However, this assay demonstrated that hemoglobin radical formation occurs in the presence of hydroperoxides, suggesting that hemoglobin radicals may be formed when cigarette smoke elicits an inflammatory response. We also showed that cigarette tar accelerates the oxidation of ascorbate when blood heme proteins (peroxidases or pseudoperoxidases) are exposed to hydroperoxides.

Bacillus subtilis reduces carcinogenic hexavalent chromate to the less-hazardous and less-water-soluble trivalent chromic form. Disappearance of chromate and a concurrent appearance of pentavalent chromium stabilized by complexation with sorbitol in the extracellular phase of metabolically active cell suspensions were demonstrated by ESR and spectrophotometric assays. This assay created the opportunity to study metabolic processes involved in the chromate reduction. Metabolic inhibitors like cyanide, potential competing anions like selenate, and the role of oxygen tension in chromate reduction were analyzed. The most striking observation was that chromate reduction could be markedly stimulated by treating the bacteria with organic "redox mediators," which appear to facilitate the flow of reducing

power from normal metabolic routes to alternative electron acceptors. A substantial fraction of the hexavalent chromium reduction product was trivalent chromium in the extracellular bulk aqueous phase which could readily be separated from the cells by centrifugation. We have proposed achromate detoxification process utilizing *B. subtilis* to effect a metal valence transformation and processed algal biomass for selectively sequestering the transformed metal species. Work is in progress to implement this technology for the remediation of chromate contaminated soils and waste waters.

References

Mehlhorn RJ, Gomez J. Hydroxyl and alkoxyl radical production by oxidation products of metmyoglobin. *Free Rad. Res. Comms.* 1993; 18: 29.

Mehlhorn RJ, Swanson CE. Nitroxide-stimulated H_2O_2 decomposition by peroxidases and pseudoperoxidases. *Free Rad. Res. Comms.* 1992; 17: 157.

Moore KL and Mehlhorn RJ. Cytostatic effects of horseradish and thyroid peroxidase derived free radicals. *Free Rad. Biol. Med.* 1993; 14: 371.

Mehlhorn RJ, Buchanan RB, Leighton T. Bacterial chromate reduction and product characterization. *Proceedings of the Second International In-Situ and On-Site Bioreclamation Symposium* (in press).

Fry IV, Mehlhorn RJ. Polyurethane and alginate immobilized algal biomass for the removal of aqueous toxic metals. In: *Proceedings of the Second International In-situ and On-site Bioreclamation Symposium* (in press).

Mehlhorn RJ. Oxidants and antioxidants in aging. In: P. Timiras, ed. *Physiological Basis of Aging and Geriatrics.* Boca Raton: CRC Publications (in press).

New Approaches to Assessing the Oceans as a Carbon Sink

M.S. Quinby-Hunt, A.J. Hunt, R. Russo

The world's oceans cover approximately 70% of the surface of the earth. The ocean provides sources and sinks for CO_2, CH_4, and other gases important to the global carbon budget. The importance of oceanic biogeochemical processes in the global carbon budget is clear, but many uncertainties remain. Not all CO_2 that is released into the atmosphere is accounted for by uptake into known terrestrial and oceanic sinks. A better understanding of the ocean's carbon budget is essential for understanding the mechanisms and kinetics of climate control.

Oceanic phytoplankton are an important component of the global carbon budget. They consume CO_2 and may release it to the water column when they decompose. After death, phytoplankton and other marine organisms decompose in the water column consuming oxygen and releasing CO_2; in regions of high productivity or low oxygen, oceanic biomass falls to the bottom and is buried in the sediments. Oxidation of biomass may cause parts of the water column and sediments to become anoxic. Many regions of the world's oceans and seas are already anoxic, for example, the Cariaco Trench off Venezuela, Norwegian fjords, and the Black Sea. Regions that are borderline anoxic are increasingly becoming more extensively anoxic including the Adriatic, portions of the Baltic Sea, and the basins of southern California. After the detritus has consumed all oxygen and sulfates, microbial and thermodynamic processes may cause formation of methane from the detritus.

Methane formed from the decomposition of phytoplankton is an important carbon sink. After formation, methane may be sequestered in hydrates (clathrates). Clathrate hydrates are solids in which water forms a rigid lattice of cages that may contain a guest molecule. In the marine environment, the guest molecule is often methane, carbon dioxide, or hydrogen sulfide (all formed during phytoplanktonic decomposition). The existence of large regions of methane clathrates on the ocean floor has been suggested based on interpretation of acoustic records: estimates report that on the order of 10^{19} g of methane exist in hydrates globally. Methane and carbon dioxide clathrates have been recovered in the Deep Sea Drilling Project and in other marine sediment cores. Clathrates can be present in marine sediments under water column depths as shallow as 70 m under cold-water conditions. Because gas hydrates form only at certain pressures and temperatures, they may be destablilized due to warming of bottom waters or changes in sea level and thereby released to the atmosphere. A significant increase in CH_4 over historical levels has been reported under sea ice off Alaska. The fate of the methane formed in the sediments may impact geochemical climate regulatory mechanisms.

Clathrates are also of interest in two additional areas: as a potential fossil fuel resource and as a submarine geohazard. If the estimate of the global resource is accurate, then the amount of organic carbon that may be stored in gas hydrates is comparable to the total quantity of organic carbon stored in other global resources. Even if the estimate is off by a factor of ten, this is a vast, untapped resource. Because the methane in gas hydrates and some of the hydrates themselves are formed in marine sediments, consolidation and cementation of the sediments can be inhibited by the presence of clathrates. The resulting structure may, therefore, be weaker and more prone to slumps, debris flows, or slides in the event of a destabilizing occurrence such as earthquakes, pressure changes due to changing sea level, or perturbation during drilling or oil/gas production activity. Clathrate-related slumps, debris flows, and slides have been reported and could present hazards to such human activities ranging from oil/gas drilling and production to communications and other cables on affected slopes.

The thermodynamics and kinetics of clathrate formation under highly reducing marine conditions are not well understood nor have the extent and stability of methane clathrates, much less clathrates of other products of phytoplanktonic decomposition, such as CO_2 or H_2S, been thoroughly investigated. A large number of potential methane clathrate occurrences have not been positively identified as instances of methane clathrates. Researchers were recently exposed to H_2S when a core which unexpectedly included hydrogen sulfide clathrates released a

toxic cloud. As the extent of marine clathrates may be great, an increased precision in the estimates of their extent would enable refinements of carbon budget models and allow better predictions of the potential impacts of clathrates on global climate regulation, their potential as fossil fuels, and the possibility that they present geological hazards.

A study of the conditions of methane clathrate formation under marine conditions was initiated at LBL. Both methane and carbon dioxide clathrates have now been prepared at LBL. Preliminary experiments were conducted using de-aerated distilled water and commercial methane and carbon dioxide. A windowed autoclave permitted observation of clathrate formation at high pressure. CO_2 clathrates were found to form readily at 900 psi and from 5-8 °C. The clathrates were brought to room temperature and pressure and removed from the autoclave to permit examination. They were found to be polycrystalline, white (similar in appearance to dry ice), and could be described as effervescent ice. Methane clathrates formed at higher pressures (~1200 psi) and at similar temperatures. In order to observe them at room temperature and pressure, it was necessary to rapidly decompress. The material retrieved was multicrystalline, and the vapor released as the clathrate evaporated could be ignited.

The chemistry and thermodynamics of formation of methane in anoxic sediments has been examined to better understand the environment under which clathrates form. The thermodynamics and kinetics of marine gas hydrates have generally been studied in distilled water in the presence of oxygen. Now that it has proven possible to form clathrates at LBL under distilled water/oxic conditions, studies are continuing under more natural conditions using water with appropriate concentrations of components found in anoxic seawater. This study will lead to a better understanding of the stability of gas hydrates and will permit a more detailed exploration of their contribution to climate regulation, their resource potential, and problems they may present as geohazards.

References

Kvenvolden KA. Gas hydrates—Geological perspective and global change. *Reviews of Geophysics* 1993; 31: 173.

Quinby-Hunt MS, Wilde P. Thermodynamic zonation in the black shale facies based on iron-manganese-vanadium. *Chemical Geology*, 1993; 112: 297-317.

Sponsors ████████████████████

██

Energy & Environment Division
Lawrence Berkeley Laboratory
University of California
Berkeley, CA 94720